

Revealing Lithium Battery Gas Generation for Safer Practical Applications

Pei Liu, Luyi Yang, Biwei Xiao, Hongbin Wang, Liewu Li, Shenghua Ye, Yongliang Li, Xiangzhong Ren, Xiaoping Ouyang, Jiangtao Hu,* Feng Pan,* Qianling Zhang,* and Jianhong Liu*

Gases generated from lithium batteries are detrimental to their electro-chemical performances, especially under the unguarded runaway conditions, which tend to contribute the sudden gases accumulation (including flammable gases), resulting in safety issues such as explosion and combustion. The comprehensive understanding of battery gas evolution mechanism under different conditions is extremely important, which is conducive to realizing a visual cognition about the complex reaction processes between electrodes and electrolytes, and providing effective strategies to optimize battery performances. This review aims to summarize the recent progress about battery gas evolution mechanism and highlight the gas suppression strategies to improve battery safety. New approaches toward future gas evolution analysis and suppression are also proposed. It is anticipated that this review will inspire further developments of lithium batteries on performance, gas suppression, and safety, especially in high energy density systems.

1. Introduction

Gas production from lithium secondary batteries received more and more attention in the recent years, especially in the struggle of developing high energy density batteries, which increases the gas evolution possibility and leads to insecurity. [1] The gases collected in battery origins from the complex reactions of all kinds

P. Liu, H. Wang, L. Li, S. Ye, Y. Li, X. Ren, X. Ouyang, J. Hu, Q. Zhang, J. Liu

Graphene Composite Research Center

College of Chemistry and Environmental Engineering

Shenzhen University

Shenzhen 518060, P. R. China

E-mail: hujt@szu.edu.cn; zhql@szu.edu.cn; liujh@szu.edu.cn

L. Yang, F. Pan

School of Advanced Materials

Peking University Shenzhen Graduate School

Shenzhen 518055, P. R. China

E-mail: panfeng@pkusz.edu.cn

B. Xiao

GRINM (Guangdong) Institute for Advanced Materials and Technology Foshan, Guangdong 528051, P. R. China

I. Liu

Shenzhen Eigen-Equation Graphene Technology Co. Ltd Shenzhen 518000, P. R. China



The ORCID identification number(s) for the author(s) of this article can be found under https://doi.org/10.1002/adfm.202208586.

DOI: 10.1002/adfm.202208586

of components contact, and the crosstalk between different parts as well as the gas consumption has a significant influence on the quantities and constituents of the gases collected,[2] making the precise analysis of gas sources and gas evolution mechanism more difficult. Side reactions between electrode materials and electrolytes are the main contributor to gases production during cycling, which is highly dependent on the types of the anode, cathode, and electrolyte applied.[1c,f,3] High specific capacity electrode materials, such as Ni-rich layered transition metal oxides (NMC),[4] Li-rich layered cathodes,[5] silicon anode,[6] and Li-metal anode, [7] are the basis of high energy density lithium battery, however, their high activity will aggravate the interfacial reactions, resulting in electrochemical performance attenuation and more gas generation.

As to the gas production analysis, researchers have carried on the studies under both normal cycling and thermal runaway conditions (Figure 1).[1c,f,4a,8] Under normal battery operating conditions, electrolyte tends to be oxidized/educed on the surface of the highly delithiated cathode/fully lithiated anode, leading to gas production, especially in the formation cycles. Later, obvious flatulence will be noticed due to the accumulated gases, [9] which may lead to capacity decay, impedance increase, material peeling from the current collector and the connection damage of cathode and anode. The series of unwanted phenomenon contributes to a decreased cycle performance and new safety risk. Furthermore, gases production will be fully enhanced under thermal runaway conditions, including a large number of flammable gases, like O₂, C₂H₄, and C₂H₆et al.^[1b,9b] Overheating is a trigger for the thermal runaway, which occurs from overcharging, [8b,10] overheating, [4a,11] external short circuits^[12] or internal short circuits,^[13] resulting in fast increase of battery internal temperature.^[1a] When the temperature reaches a certain level, the formed solid electrolyte interface (SEI) layer and separator start to decompose and melt, producing more heat and gases.[1a,14] Eventually, if the internal temperature exceeds the thermal stability temperature of cathodes, like NMC cathodes, [4a,15] oxygen release will occur to provide more combustion-supporting agent for the subsequent combustion explosion of battery. Hence, the gas formation mechanism under different conditions should be systematically summarized, which is conducive to fundamentally illustrating the

1616292. 2022, 47, Downloaded from https://advanced.onlinelibtrary.viely.com/doi/10.1002/admf.202208586 by University Town Of Shenzhen, Wiley Online Library on [2311/2025]. See the Terms and Conditions (https://onlinelibrary.wiley.com/terms-and-conditions) on Wiley Online Library or rules of use; OA articles are governed by the applicable Creative Commons License

Figure 1. Gas evolution processes under different conditions and the corresponding affection on battery performance and safety.

battery decay process and providing effective theoretical guidance for gas generation inhibition and performance optimization, and thus enhancing the development of lithium batteries with high safety.

In order to guide battery material design to enable high energy density and high safety lithium batteries, we reviewed here the gas evolution mechanism of the widely applied cathodes, anodes and electrolytes under both normal test environment and thermal runaway circumstance. The corresponding gas production processes were analyzed and summarized systematically, which is closely related to the attenuation processes of the adopted battery materials. Moreover, the gas suppression strategies were also collected and discussed, giving a comprehensive understanding for gas inhibition. Accordingly, paths for more precise gas generation analysis and measurements for effective gas suppression were proposed in the last section. This review is expected to introduce a comprehensive and clear approach to reduce gas production to enable further development of safer lithium batteries.

2. Gas Evolution from Cathodes

Cathode material is a contributor to battery capacity but a short board as well, which determines the energy density of the lithium battery, thus high specific capacity cathodes have been studied competitively. [4b] Gas generation from the cathode side is an important source of battery gases, especially under thermal runaway condition, where the gases generation will be ongoing and more gases from other components will be introduced into battery, bringing about serious safety risks. High specific capacity cathodes will enhance the above negative effects. Hence, the gas evolution mechanism from cathode side needs to be clarified and summarized in detail for safer operation, which will be shown in the following four parts.

2.1. Residue Impurities

Surface contaminants of cathode materials are an important gas source, like lithium carbonate (Li_2CO_3) on the surface of NMC cathode or Li-rich Mn-based layered cathodes. [17] It

is usually formed on the electrode surface during material preparation and storage, and has a detrimental effect on the stability of lithium batteries.^[18] The decomposition process of Li₂CO₃during battery operation has been widely studied and discussed. Nika et al. prepared carbon black/Li₂CO₃/PTFE electrode to study the decomposition products of Li₂CO₃, and found that it tends to decompose into CO₂ based on the decomposition reaction of $2\text{Li}_2\text{CO}_3 \rightarrow 4\text{Li}^+ + 4\text{e}^- + 2\text{CO}_2 + {}^1\text{O}_2$ at a relative low voltage of 3.8 V (Figure 2a).[19] Moreover, they proved that Li₂CO₃ decomposition will produce highly reactive singlet oxygen (¹O₂), which is extremely destructive to the applied electrolyte. To figure out the CO2 source in the real battery, Toru et al.^[20] labeled Li₂CO₃ with ¹³C on the surface of NMC cathode, and found that Li₂CO₃ decomposition contributes to the CO₂ generation in the first cycle. Meanwhile, the electrolyte decomposition to generate CO2 happens in the whole cycle and occupies a large proportion of the CO20bserved (Figure 2b). LiOH is also an important lithium compound on the cathode surface. which was compared with Li₂CO₃ on the gas evolution content. Lithium compounds, including Li₂CO₃ and LiOH-H₂O, were immersed into the electrolyte, which were then kept at 85 °C to monitor the gas generation behavior. The results show the chain-structured carbonates, like Ethyl methyl carbonate(EMC) and dimethyl carbonate (DMC), produced more gases than the cyclic-structured solvent (ethylene carbonate, EC), which is in contrast to the conventional expectation that the cyclic-structured solvent is less stable and would decompose through a ring-opening reaction.^[21] In short, residue lithium salts on electrode materials are recommended to be cleaned before assembled into the battery, which tends to be decomposed at high voltage state no matter in which kinds of cathodes.

2.2. Interfacial Chemical Reaction between Cathode and Electrolyte

Chemical reaction between cathode and electrolyte is the main contributor to the gases generated inside the battery, which tends to occur at higher voltages but not to the point of electrolyte electrochemical decomposition. Chemical oxidation of electrolyte is dependent on the release of reactive species, for instance, NMC releases highly reactive singlet oxygen at high voltage, which would violently react with electrolyte and

www.afm-journal.de

16163028, 2022, 47, Downloaded from https://advanced.

onlinelibrary, wiley, com/doi/10.1002/adfm.202208586 by University Town Of Shenzhen, Wiley Online Library on [23/11/2025]. See the Terms and Conditions (https://onlinelibrary.wiley.

onditions) on Wiley Online Library for rules of use; OA articles are governed by the applicable Creative Commons License

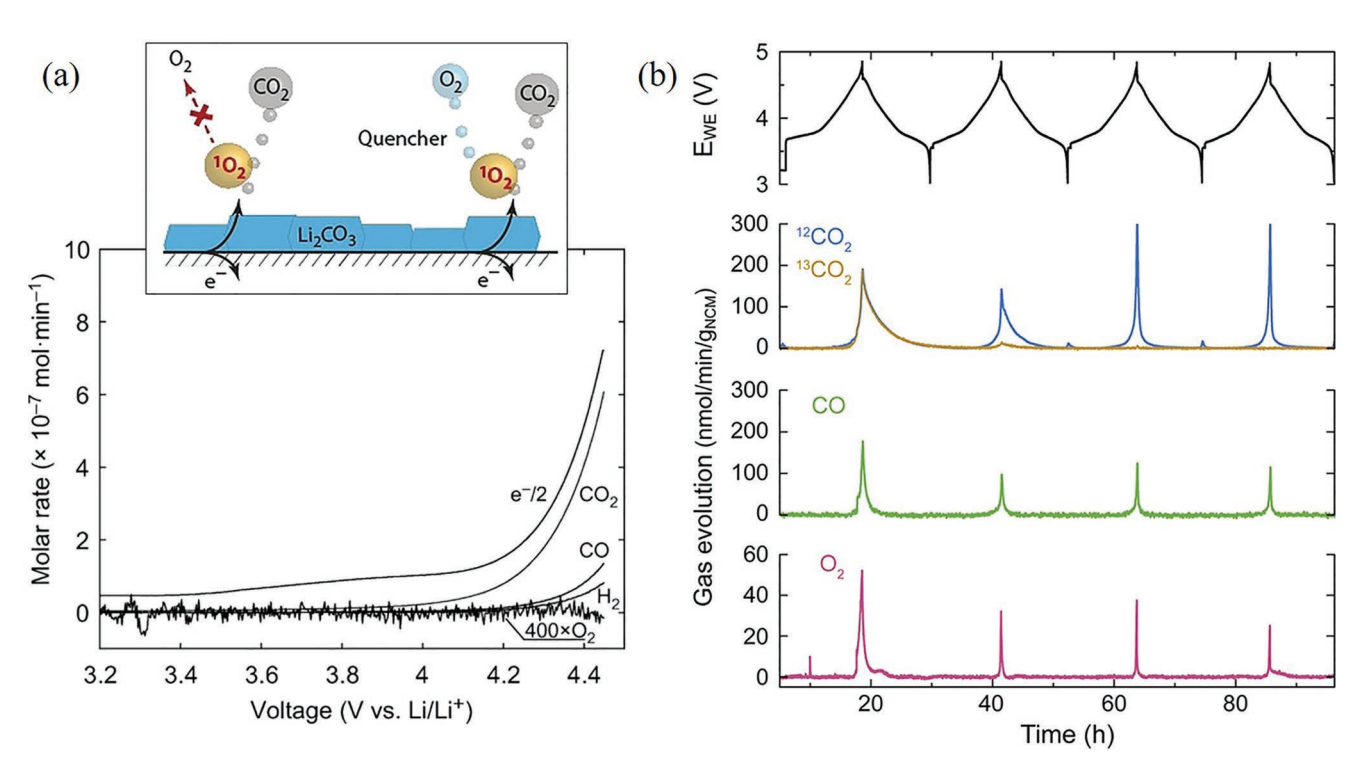


Figure 2. a) Gas evolution from carbon black/Li₂CO₃/PTFE electrodes with a scan rate of 0.14 mV s⁻¹ in 0.1 MLiTFSI in tetraethylene glycol dimethyl ether. Reproduced with permission.^[19] Copyright 2018, John Wiley & Sons. b) Voltage profile of the prepared cell and the corresponding gas evolution rates, including CO₂, CO, and O₂. Reproduced with permission.^[20] Copyright 2018, American Chemical Society.

produce gases (like CO₂, CO).^[3a] The singlet oxygen production phenomenon was proved by the comparison of NMC cathodes and Li-rich layered cathodes (LNMO), and found that it tends to occur at ≈80% state-of-charge (Figure 3a). Unavoidably, singlet oxygen formation imposes the challenge to develop high energy density lithium batteries based on layered oxide cathodes. The reaction mechanism between singlet oxygen and EC was proposed by Jung et al. as shown in Figure 3b,[22] and the corresponding reaction equation can be described as $2^{1}O_{2} + EC \rightarrow$ $2CO_2 + CO + H_2O$. [2b,16d,23] When NMC cathodes are charged beyond 4.5 V, like 4.7 V or higher, oxygen evolution will happen from the surface of the applied materials, which can be attributed to the recombination result of singlet oxygen escaped from the NMC lattice.[1c] Lithium rich compounds (LNMO) present higher specific capacity than the typical transition metal layered oxides, like NMC811, and are regarded as a promising solution toward the high-energy density lithium battery bottleneck.^[5a] However, this material suffers from serious O-loss at the particle surface for the oxidation reaction of O2- during charge process. [24] The O-loss process was extensively studied, and proved that all the charge capacity originating from Li₂MnO₃ will lead to O-loss.^[25] Hieu et al.^[26] did a comprehensive study on the structural variation of Li_{1.16}Ni_{0.19}Fe_{0.18}Mn_{0.46}O₂ (LNFM), as illustrated in Figure 3c. At the beginning of charge process, Ni²⁺ and Fe³⁺ were oxidized to Ni⁴⁺ and Fe⁴⁺ at 4.08 V, then CO₂ started to produce owing to the electrochemical decomposition of Li₂CO₃ impurity before 4.2 V. When charged to 4.55 V, the lattice oxygens are oxidized to a higher valence (superoxide radicals) and react with electrolyte to produce CO2. From 4.55 to 4.8 V, the O2 and CO2 evolution rates are increased, which correlate with the lattice oxygen release in Li₂MnO₃ and the chemical reactions between the applied carbonate solvents and reactive oxygen species, respectively. The two kinds of gases both reach to their maximum contents at the end of the first charge to 4.8 V. However, Shen et al.^[27] presented a different gas evolution mechanism, and attributed the CO₂ generation at different voltages to the strong oxidizing ability of high valence nickel ions. In general, gas evolution from the cathode side originates from the interfacial chemical reaction that is induced by the high reactive substances of cathode surface. Normally, the high reactive oxygen and high valence transition metal ions are regarded as the two contributors, but the detailed reaction processes are not well proved and clarified. Hence, high spatial and temporal resolution techniques are needed for better understanding of the gas evolution mechanism.

2.3. Thermal Runaway Condition

Thermal runaway happens at the conditions of uncontrolled exothermic reactions, including overcharging, high temperature exposure and short circuits.^[1b,1e] When the working temperature increases higher than 80 °C, more exothermic chemical reactions will follow up to further heat up the battery, leading to an undesirable feedback cycle and safety issues.^[14,28] Hence, it's significant to study the thermal runaway mechanisms for more efficient electrode material design and safer battery operation. For battery, cathode seems to be one of the most sensitive part to the temperature variation, such as NMC cathode, which tends to decompose to gases and release a lot of heat, resulting

www.afm-journal.de

16163028, 2022, 47, Downloaded from https://advanced.onlinelibrary.wiley.com/doi/10.1002/adfm.202208586 by University Town Of Shenzhen, Wiley Online Library on [23/11/2025]. See the Terms and Conditions (https://onlinelibrary.wiley

onditions) on Wiley Online Library for rules of use; OA articles are governed by the applicable Creative Commons

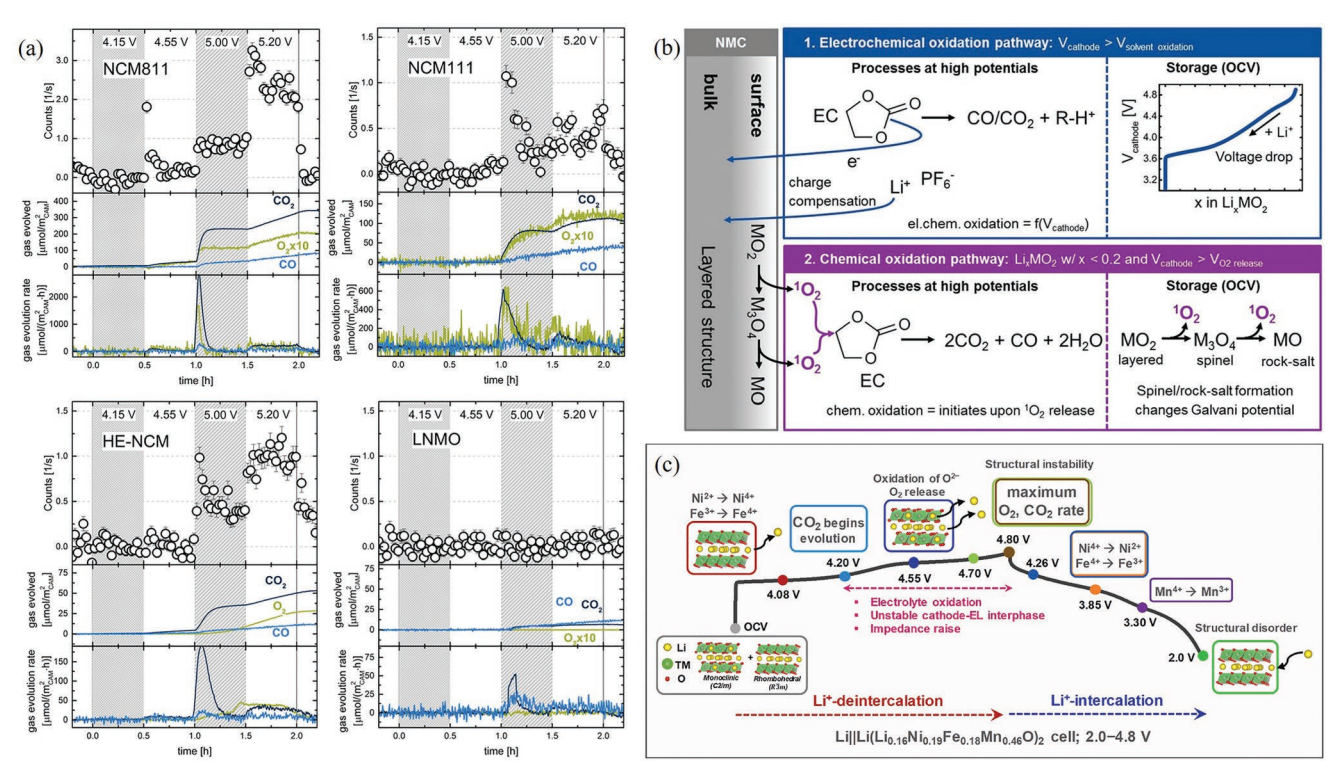


Figure 3. a) Gas evolution comparison of NCM811, NCM111, over lithiated NCM (HE-NCM) and LNMO tested in 1 M LiPF₆ in EC/EMC (3:7 by volume). Reproduced with permission. ^[3a] Copyright 2018, Elsevier. b) Schematic illustration of the possible electrochemical and chemical electrolyte oxidation paths. Reproduced with permission. ^[22] Copyright 2017, Elsevier. c) Proposed mechanism of the reaction processes of Li-rich and Mn-rich layered oxide cathode when charged to 4.8 V, including structure evolution, gas production and interfacial reaction. Reproduced with permission. ^[26] Copyright 2022, Elsevier.

in battery expansion and heat accumulation.[1e,4a,15a,29] Seong-Min et al.[29] studied the thermal decomposition processes of the overcharged layered cathodes by the combination of timeresolved synchrotron X-ray diffraction and mass spectroscopy. The structural changes of the cathode are correlated with the evolution of the captured gas, as illustrated in Figure 4a. It is clear that the evolution of O2 and CO2 from the delithiated LixN i_{0.8}Co_{0.15}Al_{0.05}O₂ can be attributed to the phase transitions from layered structure to the disordered spinel structure and finally to the rock-salt structure. In particular, they noticed that the degree of the charge state affects both the phase transition temperature and the oxygen release temperature significantly. For better understanding the thermal stability of NMC cathodes, Seong-Min and co-authors^[15a] systematically investigated the structural variation and gas production of NMC433, NMC532, NMC622, and NMC811, and found that NMC532 composition presents an optimal performance (Figure 4b). By comparing the above four materials, it's noticed that Ni is the least stable element and experiences the fastest reduction from Ni⁴⁺ to Ni²⁺ during the thermal decomposition, hence it can be concluded that the Ni⁴⁺ content after charge governs the thermal stability of NMC cathodes. In contrast, Mn and Co plays an important role in improving and maintaining the thermal stability of materials, respectively. Moreover, the phase stability map of the charged NMC with different Ni content is obtained and presented in Figure 4c, which directly expresses the structural stability of NMC at different charge states.^[15a] M. Guilmard et al.^[30] investigated the thermal degradation mechanism of LixNi1.02O2

and $\text{Li}_x \text{Ni}_{0.89} \text{Al}_{0.16} \text{O}_2$, and proved that the two materials own the same degradation mechanism, which mainly consists of two steps: layered structure to pseudo-spinel transformation and the progressive transformation to NiO-type structure accompanied with O-loss. Moreover, the thermal stabilization is enhanced by the Al substitution for Ni (Figure 4d), which can be explained by the stability of the Al^{3+} ions in tetrahedral sites disrupting the cationic migrations. Accordingly, suppressing the surface phase variation of cathodes is an important way to improve the thermal stabilization and safety of battery. Methods including locking lattice oxygen and fixing transition metals, are recommended, and the corresponding routes will be presented in the following sections.

2.4. Influence of Other Components of Electrode

The regulation of electrode drying process and material storage environment is very important for improving the electrochemical performance by eliminating the residue water. The residue water within electrode will diffuse into electrolyte, which not only destroys the electrolyte environment, but also contributes to more $\rm H_2$ generation by its reduction reaction at the anode side. It will be further illustrated in the next section. Carbon black is an indispensable part of the electrode, which can also contribute to the gas evolution, especially under the high voltage conditions. [16d,31] For instance, Michael et al. [32] analyzed the corrosion of conductive carbon (Super C65) and PVDF binder at

16163028, 2022, 47, Downloaded from https

onlinelibrary.wiley.com/doi/10.1002/adfm.202208586 by University Town Of Shenzhen, Wiley Online Library on [23/11/2025]. See the Terms

on Wiley Online Library for rules of use; OA articles are governed by the applicable Creative Commons

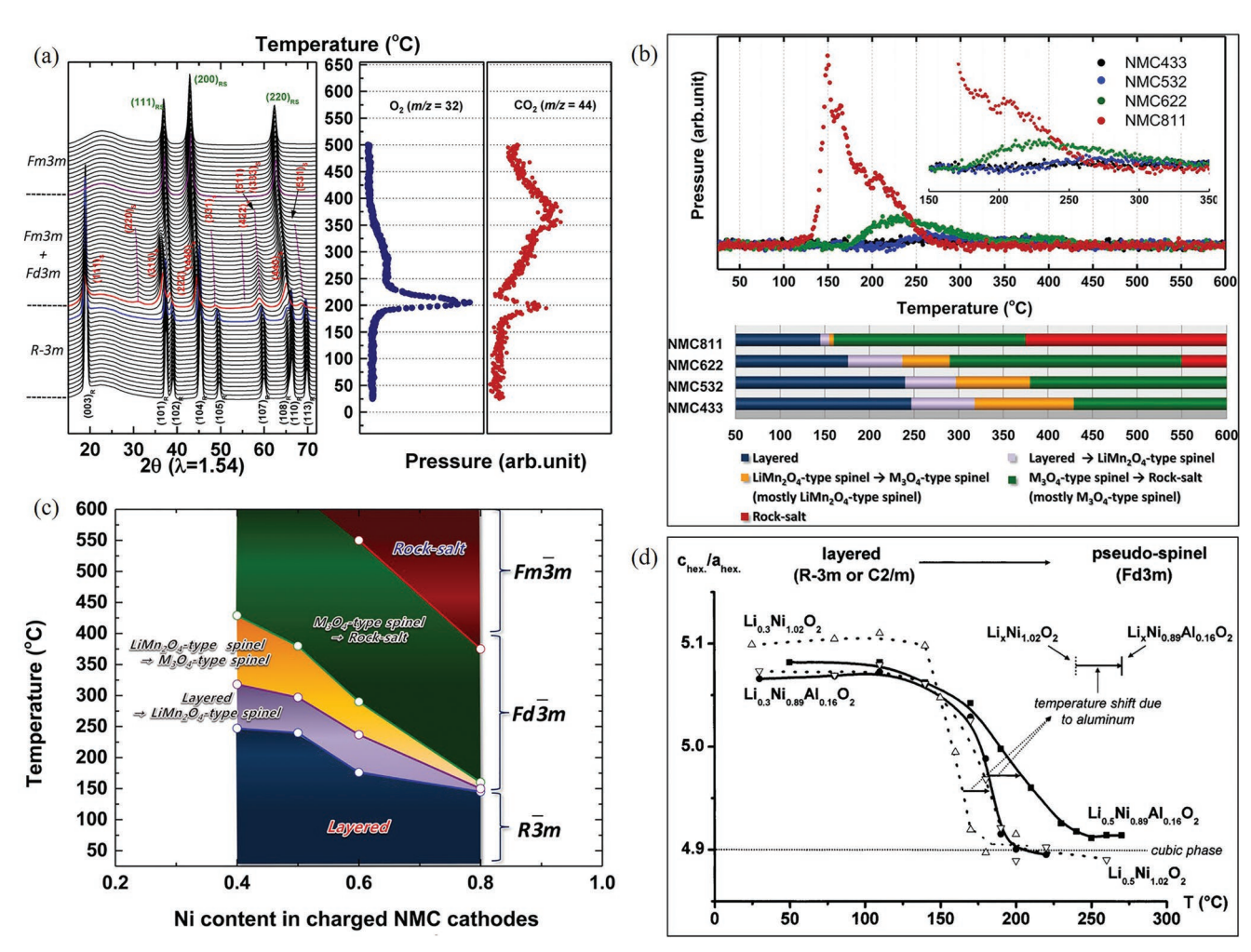


Figure 4. a) The structure variation and gas evolution results of $\text{Li}_{0.1}\text{Ni}_{0.8}\text{Co}_{0.15}\text{Al}_{0.05}\text{O}_2$ during heating to 500 °C. Reproduced with permission. [29] Copyright 2013, American Chemical Society. b) Mass spectroscopy profiles of oxygen obtained during the heating process to 600 °C, and the lower panel shows the corresponding phase transitions of the NMC samples during heating. Reproduced with permission. [15a] Copyright 2014, American Chemical Society. c) The phase stability of the charged NMC cathodes during heating. Reproduced with permission. [15a] Copyright 2014, American Chemical Society. d) Evolution of the c/a ratio changed with the increasing of temperature of $\text{Li}_{v}\text{Ni}_{1.02}\text{O}_{2}$ and $\text{Li}_{v}\text{Ni}_{0.89}\text{Al}_{0.16}\text{O}_{2}$. Reproduced with permission. [30] Copyright 2003, American Chemical Society.

high cutoff voltage by using a fully isotope labeled EC-based electrolyte (referred as ¹³C₃EC), which is an essential component in the commercial electrolytes. They found that conductive carbon produced lots of gases in the presence of trace water or/and functioned in high temperatures (Figure 5a,b). Carbon coating strategy is widely applied for cathode materials with low intrinsic electrical conductivity to improve their electrochemical performance, like olivine structure LiMPO₄ (M equals to 3d-transition metal). However, the carbon coating layer may experience anodic oxidation at high voltage and produce gases in the presence of water. Michael et al.[33] systematically studied the affection of working voltage and water content on the gas production from LiFePO₄ based batteries, and the corresponding carbon coating layer was isotopically labeled ¹³C. They found that the oxidation of carbon coating layer happens when the potential is higher than 4.75 V in the water-free electrolyte, or 4.5 V in the electrolyte with 4000 ppm water, and the gas content in the water-contained electrolyte is larger than that in the water-free electrolyte. (Figure 5c) Moreover, Michael et al.[34] compared the oxidation stability of conductive carbon in organic electrolytes coupled

with different lithium salts, including LiClO₄, LiPF₆, and LiTFSI under various temperatures between 25 and 60 °C. By analyzing the CO/CO₂ data, they captured the decomposition of conductive carbon at high voltage and noticed that the molar oxidation rates at different electrolytes are different, which elucidates the importance of lithium salts on gas generation at high voltage and provides guidance to the design principles for novel electrolytes. For practical research of battery applications, a dry experimental circumstance is necessary, and the functions of voltages and electrolyte salts should be well controlled to exclude the gas interference generated from the conductive carbon, which is significant to get the gas evolution mechanism accurately.

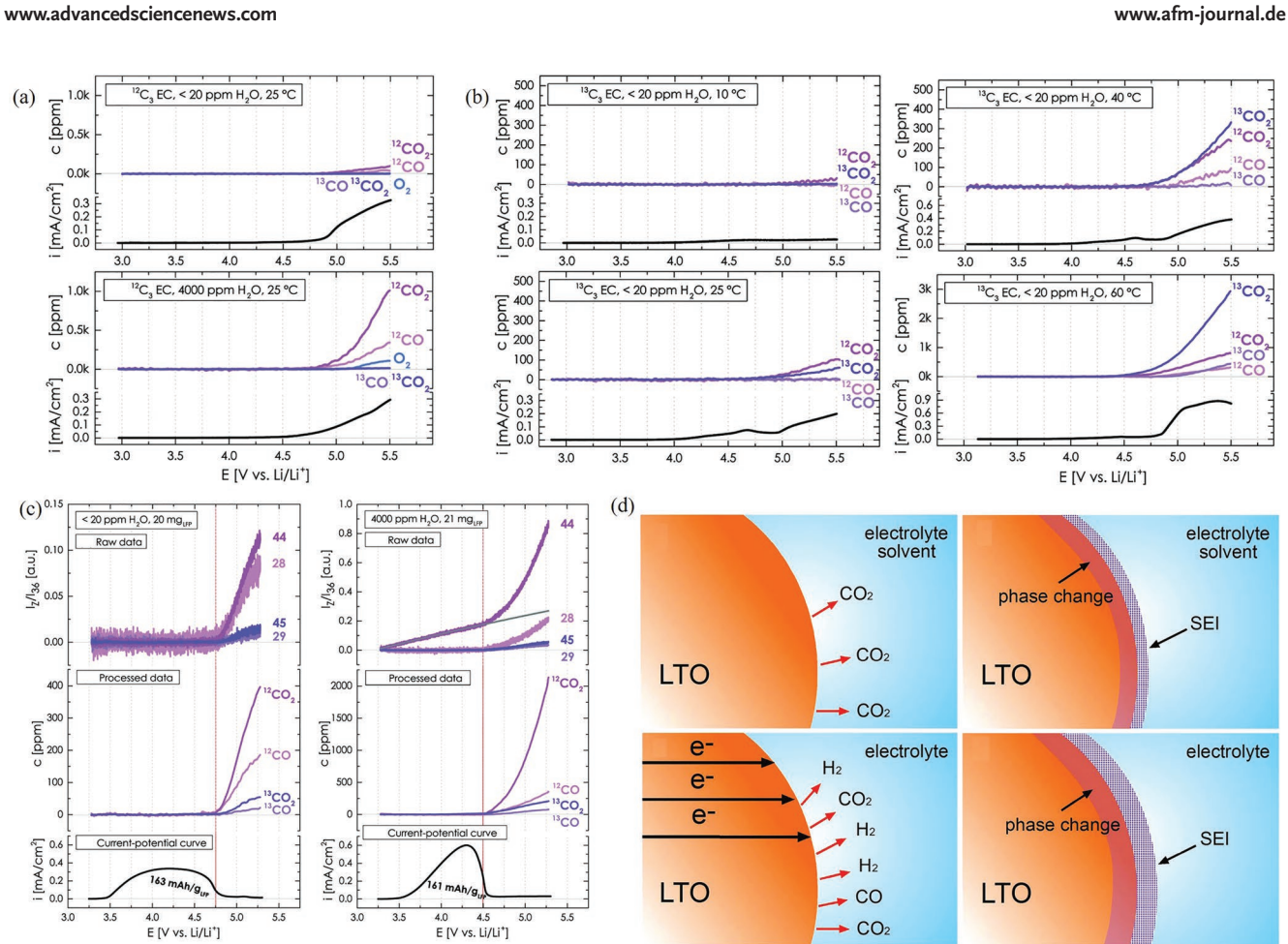
3. Gas Evolution from Anodes

Anode is coupled with cathode to run a battery, which experiences low potential environment and its surrounding substances are easy to be reduced, including the formed solid electrolyte interphase (SEI), contaminants, electrolyte, et al. Based on the

16163028, 2022, 47, Downloaded from https://adv

nlinelibrary.wiley.com/doi/10.1002/adfm.202208586 by University Town Of Shenzhen, Wiley Online Library on [23/11/2025]. See the Terms

ditions) on Wiley Online Library for rules of use; OA articles are governed by the applicable Creative Commons



25°C Li₄Ti₅O₁₂ Only electrolyte " E 150°C $TiO_2 + CO_2 + C_2H_5OC_2H_5 + CH_2CO_2Li$ Rutile TiO₂ volume / (-CH₂-CH₂-O-)_n + n CO₂ gases v 1M LIPF JEMC IM LIPF (DEC M LIPF /DMC 1M LIPF /PC CO2 + 2Li+ + 2e-- CO + Li₂CO₂ Condition

Figure 5. a) Voltage-dependent CO2, CO, and O2 evolution during the oxidation of a Super C65/PVDF electrode in H2O-free and 4000 ppm H2Ocontaining electrolytes when charged to 5.5 V at 0.2 mV s⁻¹. Reproduced with permission [32] Copyright 2015, Elsevier. b) The affection of temperature on CO₂and CO production of Super C65/PVDF electrode when charged to 5.5 V at 0.2 mV s⁻¹. Reproduced with permission. [32] Copyright 2015, Elsevier. c) The oxidation results of coating carbon in the presence of different contents of water in the applied organic electrolyte, the corresponding working electrode and counter electrode are LiFePO₄@C and Li-metal, which was charged to 5.3 V at 0.05 mV s⁻¹. Reproduced with permission. [32] Copyright 2015, Elsevier. d) CO2 production on the surface of LTO without and with SEI layer (upper plane). Gaseous H2, CO2 and CO are produced from LTO surface without and with SEI layer coupled with NMC cathode. Reproduced with permission. [38] Copyright 2015, Springer Nature. e) Gas evolution content of LTO and rutile TiO2 under different conditions. Reproduced with permission. [38] Copyright 2015, Springer Nature. f) Proposed gas generation reactions in the gassing LTO electrode. Reproduced with permission. [38] Copyright 2015, Springer Nature.

previous literatures, the gas evolution mechanism from anode side is reviewed and demonstrated by the following four aspects.

3.1. Electrolyte Reduction

(e)

The widely applied negative electrode in lithium batteries is graphite due to its stable structure with high theoretical capacity (372 mAh g⁻¹) and low working voltage as well as limited interfacial reaction. In practical applications, there are many gases generated from the graphite surface owing to the electrolyte reduction companied with the formation of SEI. One of the most dominated gas is ethylene (C2H4), which can be attributed to the electrolyte reduction under the voltage of 0.8 V,[2b,35] and the corresponding decomposition processes can be illustrated as $2EC + 2Li^+ + 2e^- \rightarrow C_2H_4 + (CH_2OCO_2Li)_2$ and $EC + 2Li^+ +$ $2e^- \rightarrow C_2H_4 + Li_2CO_3$. [36] Rebecca et al. studied the C_2H_4 generation mechanism by comparing the gas evolution results in

1616292. 2022, 47, Downloaded from https://advanced.onlinelibtrary.viely.com/doi/10.1002/admf.202208586 by University Town Of Shenzhen, Wiley Online Library on [2311/2025]. See the Terms and Conditions (https://onlinelibrary.wiley.com/terms-and-conditions) on Wiley Online Library or rules of use; OA articles are governed by the applicable Creative Commons License

FUNCTIONAL

 H_2O -free and 4000 ppm water organic solutions, and proved that the formation of C_2H_4 is from the water free electrolyte by the reduction of EC. $^{[35]}$ CO is another product from the EC reduction, and the detailed decomposition pathway was proved to be a two-electron reaction as EC + 2Li^+ + 2e^- \rightarrow (CH₂OLi)₂ + CO. $^{[37]}$ More detailed information will be illustrated in the electrolyte decomposition section.

The interfacial reaction between lithium titanate (LTO) anode and the electrolyte results in more gases compared to graphite anode owing to its un-protected surface with high activity. In LTO system, the redox potential is 1.55 V versus Li/Li+, which is higher than that in graphite-based batteries, and the gas production content is supposed to be less due to missing the low voltage stage. However, the interfacial parasitic reaction between LTO and electrolyte tends to happen in the whole electrochemical process owing to the naked surface, which leads to a constant gas production and electrochemical performance attenuation. He et al.[38] did a comprehensive study on the gas evolution of LTO-based batteries and found that the generated gases mainly contain H2, CO2 and CO, which are initiated by the decarbonylation, decarboxylation, and dehydrogenation reactions of solvents on the outermost LTO (111) plane (Figure 5d,e). At the end of the gas production, the reaction basal of (111) plane transforms to (222) plane, and the Li+ and O²⁻ ions are removed from the surface of (111) plane by the interfacial reactions. The main reaction mechanism is shown in Figure 5f that CO2 is generated by the decarboxylation reaction of organic solvents, the alkoxy groups in alkyl carbonates dehydrogenate to H₂ under the catalytic action of LTO, and the intermediate of solvent dehydrogenation can also accept electron and Li⁺ for decarbonylation to form CO. Moreover, in this system, CO₂ can also be reduced to CO. Gas analysis shows that H₂was produced together with other gases, most of which was attributed to the side reaction of electrolyte and contaminant on LTO surface catalyzed by Ti-O bond in LTO.[39]

3.2. SEI Decomposition

SEI is a perfect protection layer on the surface of the anodes. like graphite and silicon, which initially forms during the first formation cycle and owns the ability to suppress the interfacial parasitic reactions with the electrolytes. Normally, SEI layer is stable on the surface of anodes, however, it may encounter morphology break by the wild volume variation or decomposition reaction under thermal runaway condition. The broken SEI layer contributes to more interfacial reaction and results in more gases, which tends to occur in the whole electrochemical process, especially when there is a large volume change during lithiation and delithiation, such as silicon. At high temperature, SEI layer decomposition can be observed and accompanies with some exothermic reactions, [40] which not only leads to the capacity decay, power attenuation and gas evolution, [41] but also increases the possibility of thermal runaway and exacerbates the safety risk. Li₂CO₃ has been observed to be a major constituent of the SEI formed on graphite electrode, [36a] which may experience decomposition to generate CO₂under the condition of high temperature. There are numerous articles about the thermal behavior of SEI,[42] and it has been reported that the exothermic decomposition of SEI at about 100—150 °C can lead to the thermal runaway of lithium ion batteries.[43]Taeho et al.[44] studied the SEI thermal decomposition process on silicon electrode by monitoring the disintegration of lithium ethylene dicarbonate (LEDC), because they have very similar thermal decomposition processes. The thermal decomposition process of model SEI (LEDC) has three stages, where LEDC decomposes into CO₂ and C₂H₄, leaving lithium propionic acid (CH₃CH₂CO₂Li) and Li₂CO₃ as solid residues when the temperature increases from 50 to 300 °C. In the heating process from 300 to 600 °C, CH₃CH₂CO₂Li decomposes into pentanone, leaving Li₂CO₃ as a residual solid. Finally, Li₂CO₃ breaks down beyond 600 °C and evolves into CO2, leaving lithium oxide as a residual solid (Figure 6a). The thermal behaviors of lithiated graphite were studied in 1 MLiPF₆-EC/DMC electrolyte, wherein CO2 evolution was observed owing to the partial destruction of the formed SEI consistence with the small exothermic peak around 140 °C. [45] The broken SEI results in alarge exothermic peak above 280 °C caused by the drastic side reaction between the lithiated graphite and the electrolyte applied, which promotes the formation of C₂H₄O. Liu et al.^[8a] studied SEI decomposition, lithium leaching and gas evolution of the lithiated graphite under the high temperature circumstance, and emphasized the importance of robust SEI and coating layer construction. Under normal operation, the electrochemical reduction process is the main contributor to the gas production. In contrast, at high temperature, the plated or the leaching metal lithium on the anode surface will react with SEI components and PVDF binder to produce gases. Hence, to minimize the possibility of electrolyte reduction, an excellent barrier is needed between electrolyte and anode, which can be a dense coating layer or a robust SEI layer. Moreover, further efforts on tuning lithium nucleation process on the anode surface are also suggested for reducing safety risks caused by metal Li.

3.3. Contaminants Reduction

Contaminants in the electrolyte or/and anode electrode, contribute to more gases driving from the reduction process on the anode surface. H2O is one of the most important contaminants within the cell, which is generated mainly by the insufficient drying or the parasitic reaction. Bernhard et al.[17b] used differential electrochemical mass spectrometry (DEMS) to clarify the decomposition process of H₂O, which was proposed to be a single electron process as $H_2O + e^- \rightarrow OH^- + 0.5H_2$. Wu et al. [46] believes that moisture is the main cause of battery flatulence. They prepared electrolytes with different water contents to simulate the effect of water on the gas production in LTO||Li(Ni_{1/3}CO_{1/3}Mn_{1/3})O₂ flexible battery. The results show that the expansion rate increases with the increase of the injected water. During the initial formation cycle, the water in the graphite electrode decomposes to H2near the potential of 1.2 V, and the water absorbed in the LTO electrode still exists after formation, mainly because the working potential of LTO is higher than 1.3 V versus Li/Li+. However, the residual water will react with PF₆⁻ in the electrolyte to form POF₃, ^[47] which is believed to catalyze the decomposition of carbonate and then produce CO₂. Moreover, the existence of water inside the battery

www.afm-journal.de

16163028, 2022, 47, Downloaded from https://adv

anced.onlinelibrary.wiley.com/doi/10.1002/adfm.202208586 by University Town Of Shenzhen, Wiley Online Library on [23/11/2025]. See the Terms

onditions) on Wiley Online Library for rules of use; OA articles are governed by the applicable Creative Commons

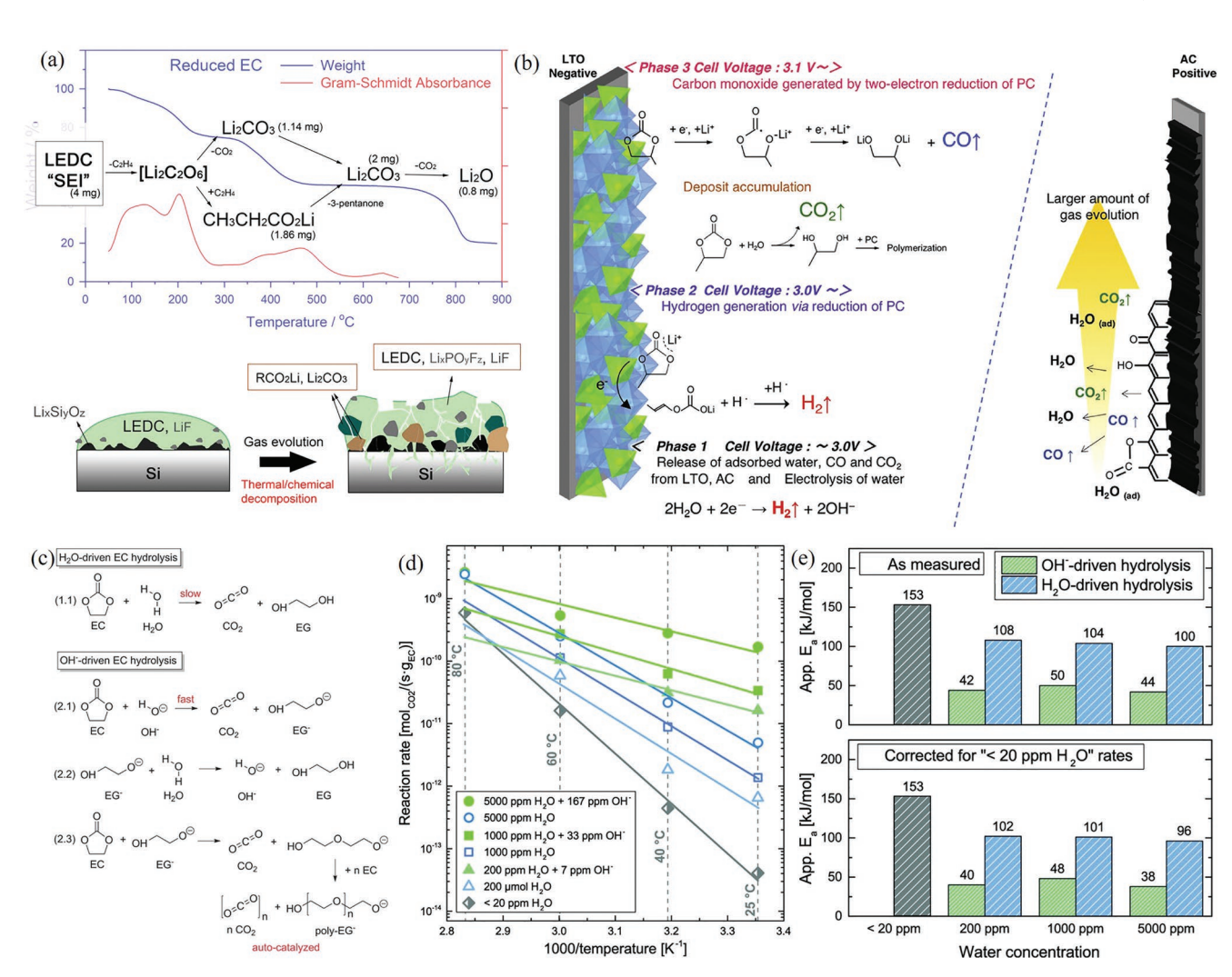


Figure 6. a) The thermal decomposition mechanism of LEDC and illustration of SEI composition change during cycling on the surface of Si electrode. Reproduced with permission. [44] Copyright 2017, American Chemical Society. b) Gas generation in LTO[1 $\,$ MLiBF $_4$ in PC[AC hybrid supercapacitor cells at different voltages. Reproduced with permission. [47] Copyright 2019, Elsevier. c) The possible EC hydrolysis routes driven by H $_2$ O and OH $^-$. Reproduced with permission. [52] Copyright 2013, Elsevier. d) Arrhenius plot of EC-normalized CO $_2$ evolution rates by the decomposition of EC at different concentrations of H $_2$ O and OH $^-$. Reproduced with permission. [52] Copyright 2013, Elsevier. e) The activation energy of EC hydrolysis by the catalytic of H $_2$ O and OH $^-$ at different water concentrations. Reproduced with permission. [52] Copyright 2013, Elsevier.

will accelerate the occurrence of H2generation, and promote the subsequent formation of hydrogen, such as the decomposition of propylene carbonate (PC) (Figure 6b)[48] To figure out the origin of H₂ (from the decomposition of H₂O or organic electrolytes), Fell et al.^[49] added different contents of heavy water (D₂O) into the electrolyte and electrode. They found that in addition to D₂, there were H₂ and DH components in the collected gases. The more heavy water (D2O) content was, the more H2 and DH (H-D products) were produced. D element in DH comes from D₂O, while H element comes from ester solvent, which indicates that OD⁻ generated by decomposition of residual water in the battery will participate in the subsequent reaction of ester to generate DH. In the same year, He et al.[50] certificated that H₂ was mainly derived from water decomposition that occurred in the early cycles. Rebecca et al.[51] used electrolytes with different water contents (20 ppm, 4000 ppm, and 4%) to analyze the gases in LTO-based batteries, including LTO||LiFePO4 and LTO||Li cells. When the water content is 20 ppm, the volume

of gases generated from the LTO is very low. However, with the condition of 4000 ppm and 4% H₂O, the water reduction on the surface of LTO is enhanced and produces lots of H₂ and OH⁻. The formed hydroxide ions facilitate the EC decomposition as shown in equation of OH⁻ + EC \rightarrow C₂H₅O₂⁻ + CO₂. [17b,52] Moreover, the hydrolysis reaction between H2O and EC was also detected by Michael and his colleagues, that the reaction of EC with trace amounts of water was strongly accelerated, especially at 60 °C, resulting from the enhanced oxidation effect of conductive carbon and electrolyte. [32] The corresponding hydrolysis reaction can be demonstrated as $H_2O + EC \rightarrow (CH_2)_2(OH)_2 +$ CO₂. According to the above analysis, it's well known that H₂O and OH- drive EC hydrolysis to produce many unexpected substances, including gases. However, it is not clear how the existence of OH⁻ affects the decomposition efficiency of EC by H₂O. Michael and co-authors studied the CO2 evolution rate of EC in the absence and presence of catalytically active OH⁻ at various temperatures (10-80 °C) and water concentrations (<20 ppm,

www.afm-journal.de

1616292. 2022, 47, Downloaded from https://advanced.onlinelibtrary.viely.com/doi/10.1002/admf.202208586 by University Town Of Shenzhen, Wiley Online Library on [2311/2025]. See the Terms and Conditions (https://onlinelibrary.wiley.com/terms-and-conditions) on Wiley Online Library or rules of use; OA articles are governed by the applicable Creative Commons License

200, 1000, and 5000 ppm H_2O), and proved that OH^- is a much stronger nucleophile than H_2O and contributes more gas production (Figure 6c–e).^[52] It's clear that H_2O , as the main component of commercial electrolyte, has an unfriendly influence on EC, which promotes EC decomposition to generate gas. Moreover, the H^+ and OH^- products are also not welcome in the organic electrolytes. Accordingly, the H_2O -free electrolyte is highly required, and the EC-free electrolyte should be recommended in the future lithium batteries.

3.4. Cross-Talk Reactions

The gases detected from lithium batteries are usually comprehensive results, and only parts of them are produced from the cathode side or the anode side as illustrated in the above section. Hence, the interaction effect between the two electrodes should also be considered, where the products (like evolved gases, decomposition products et al.) from one electrode can be absorbed or consumed at the other to generate more substances. In principle, the evolved gaseous products and oxidized substances can scatter on the surface of positive electrode and/ or dissolve in the electrolyte, which, however, can also reach to the negative electrode and be reduced there.^[53] H₂ evolution has been seen to be an important cross-talk reaction.[1c,2b,54] For instance, Michael et al. [2b] found that Graphite||NMC cell without any buffer layer between cathode and anode shows enhanced H₂ generation, and they proposed that there is a substance named as protic electrolyte oxidation species (R-H⁺), which diffuses from the cathode to the anode to be reduced for an increase of H₂ production. This hypothesis was successfully proved by adding methanesulfonic acid in the electrolyte as a chemical source of protons, which were quantitatively reduced to H₂. Moreover, the authors introduced an Al-sealed diffusion barrier between anode and cathode to stop the R-H⁺ diffusion. as expected, this design essentially eliminates that the generation of H₂was caused by the high cathode potentials.

Carbon dioxide consumption is one of the most significant consumption reactions in lithium batteries. When the tested batteries coupled with lithium metal anode, the produced CO₂ tends to react with lithium metal to form carbon deposits coating on the anode surface.^[55] Graphite anode can be regarded as a sink for CO_2 produced from the cathode side, [2a,f] which is easily consumed to form lithium oxalate.^[56] This "conversation" between the two electrodes has been proposed to create a "shuttle" that could harm battery performance. [2e] To figure out the relationship of gas evolution and subsequent consumption, Ellis et al. carried out a comprehensive study by using Archimedes' principle and gas chromatography, and found that except the aforementioned CO2 and saturated hydrocarbons, all the evolved gases are subsequently consumed at the anode side and reduced to form the SEI layer (Figure 7a). [56] In addition, the cross-talk reaction also relates to the soluble products. For example, the cathodes containing transition metals may experience the dissolution (especially Mn²⁺), resulting in their deposition on the surface of the formed SEI, which could damage the graphite SEI surface and induce enhanced electrolyte reduction and more gases. Michalak et al.[57] compared the gas generation content in graphite||LiNi_{0.5}Mn_{1.5}O₄ with that in

LTO||LiNi $_{0.5}$ Mn $_{1.5}$ O $_4$ cells, and found that LiNi $_{0.5}$ Mn $_{1.5}$ O $_4$ electrode produced more gases when coupled with graphite anode than LTO electrode (Figure 7b,c), which can be explained by the unstable SEI interface induced by the deposited transition metals. The above-mentioned cross-talk reactions have been detected and reported already, and it's reasonable to infer that there are more cross-talk reactions that have gone undetected. Hence, more in situ and high-resolution techniques are needed to visualize the whole reaction processes of electrodes in real-time in battery.

4. Electrolyte Decomposition for Gas Evolution

Electrolyte has been described as the "blood" of lithium batteries, which is not only responsible for the ion transfer between cathode and anode, but also inhibits the parasitic reaction at the electrode/electrolyte interface by building a protective layer to enable high performance for lithium batteries.^[58] However, the electrolytes widely applied now have two sides, which are judged to be responsible for the battery safety issue owing to their flammability and gas production, especially under unguarded thermal runaway conditions. It is well known gas production mainly originates from the decomposition of solvents and the corresponding reaction products such as SEI, hence a detailed conclusion about the gas evolution mechanism from electrolytes would be of great significance. The contribution of all kinds of electrolytes for high energy density lithium batteries, including organic liquid electrolytes, solid-state electrolytes, and polymer electrolytes et al., are reviewed as follows.

4.1. Conventional Organic Liquid Electrolyte

Solvent, salt and additive are the three components of the traditional liquid electrolyte, and the corresponding combination form is closely related to the gas categories and gas content. Ester solvents mainly include circular carbonates (e.g., EC, PC) and chain carbonates (e.g., EMC, DMC). EC is the most important gas contributor and certainly has received extensive studies. Generally, there are three pathways causing EC decomposition and producing gases, including cathode/EC interface reaction, anode/EC interface reaction and impurity affection. At a high charge state of cathode, EC would be oxidized and present as ring opening reaction accompanied with CO2 and CO evolution. [1c,2b,3a] The detailed decomposition reaction of EC ring opening was proposed by Hubert and co-authors, [2b] as shown in Figure 7d, which is a chemical reaction pushed by the released strong oxidizer from cathode materials (e.g., singlet oxygen) and their high active surface. Normally, the solvents applied in electrolyte are stable under 5 V, so the collected gases should not be from the simple electrochemical decomposition of EC.[1c,3a] At anode side, EC would be electrochemically reduced by receiving electrons under certain potentials, and the corresponding by-products include lithium ethylene dicarbonate (LEDC), C2H4, and CO et al. [59] CO2 and H2 were also observed. [2b,59] As to CO2, it was regarded as the reaction product between EC and POF₃,^[50,60] however, the generated CO₂ experienced continuous consumption at low potentials^[2e,59]

www.afm-journal.de

16163028, 2022, 47, Downloaded from https://advanced.onlinelibrary.wiley.com/doi/10.1002/adfm.202208586 by University Town Of Shenzhen, Wiley Online Library on [23/11/2025]. See the Terms

onditions) on Wiley Online Library for rules of use; OA articles are governed by the applicable Creative Commons

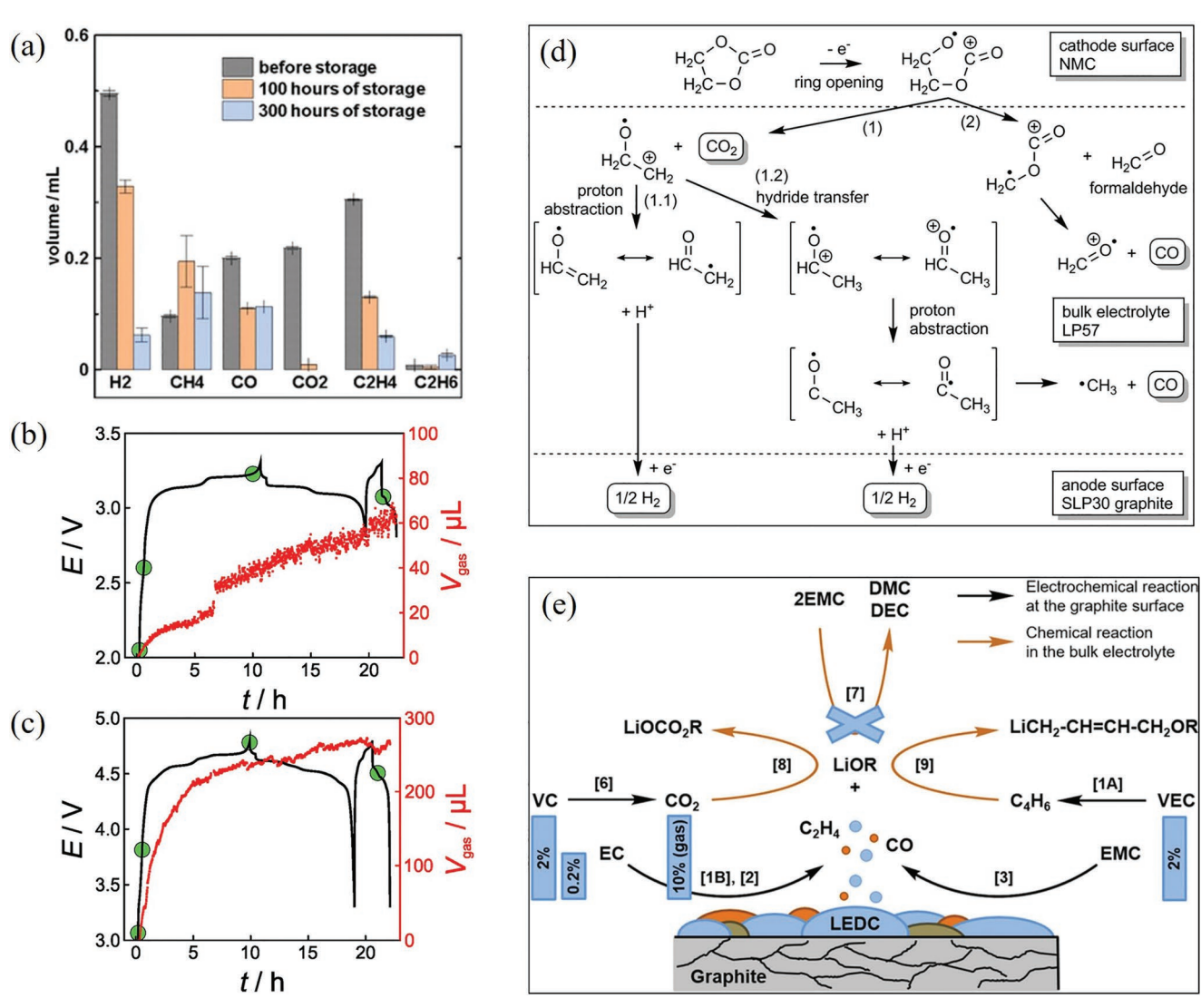


Figure 7. a) Variation of gas content of the 4.5 V charged fresh cells at different storage time. Reproduced with permission. [56] Copyright 2017, Electrochemical Society. b) Voltage and gas volume profiles of LTO||LiNi_{0.5}Mn_{1.5}O₄ cell. Reproduced with permission. [57] Copyright 2015, Springer Nature. c) Voltage and gas volume profiles of graphite||LiNi_{0.5}Mn_{1.5}O₄ cell. Reproduced with permission. [57] Copyright 2015, Springer Nature. d) Proposed mechanism of EC decomposition and its contribution to the CO₂, CO and H₂ evolution. Reproduced with permission. [2b] Copyright 2016, Electrochemical Society. e) Schematic description of the interface formation processes, the VC and VEC decomposition were also included. Reproduced with permission. [61] Copyright 2017, Electrochemical Society.

that should be considered during gas content quantification. H_2 production was systematically studied by Hubert, $^{[2b]}$ and concluded that H_2O contamination and protic electrolyte oxidation species (R-H⁺) from the cathode are the main contributors to the H_2 evolution at anode side. Water and hydroxide promote EC hydrolysis was studied by Hubert and co-authors, demonstrating that OH^- -driven EC hydrolysis happens at room temperature and H_2O -driven EC decomposition is only relevant at elevated temperature (\geq 40 °C) (Figure 6c), $^{[52]}$ Other solvents, like EMC, PC and DMC, also contributed to the gas evolution during electrochemical process, that EMC contributes to CO production, $^{[61]}$ and in PC-based electrolytes, $^{[62]}$ CO₂, CO and C_3H_8/C_3H_6 are the characteristic gases. As to DMC solvent, it promotes the generation of CH_4 . $^{[62]}$ In short, the molecular structural formula of the applied solvents in electrolytes and

the corresponding bonding energy are important references to understand the gases generation behavior of batteries.

Salt selection also has great influence on the gas generation, as illustrated by Michael and co-authors^[63] that lithium tetrafluoroborate (LiBF₄) presents excellent electrolyte stability at high temperature (50 °C) and high voltage (5 V) at cathode side, as compared to LiClO₄, LiPF₆ and lithium bis(trifluoromethane)-sulfonimide (LiTFSI). However, LiPF₆ and LiTFSI show pronounced advantage on the gas suppression of conductive carbon under the above extreme conditions. LiClO₄ seems to be the worst choice that amounts of gases were generated from both carbon and electrolyte over all temperature ranges, especially at high temperature. Oxygen containing gas POF₃ is noticed in case of the LiPF₆-based electrolyte solutions, and its generation process is believed to obey this

16163028, 2022, 47, Downloaded from https://advanced.onlinelibrary.wiley.com/doi/10.1002/adfm.202208586 by University Town Of Shenzhen, Wiley Online Library on [23/11/2025]. See the Terms and Conditions (https://onlinelibrary.wiley.com/

and-conditions) on Wiley Online Library for rules of use; OA articles are governed by the applicable Creative Commons License

ADVANCED FUNCTIONAL MATERIALS

equation (PF₅ + H₂O \rightarrow POF₃ + 2HF), nevertheless, PF₅ may originate from different sources, including LiPF₆ \leftrightarrow LiF + $PF_5^{[64]}$ and $EC + H_2O \rightarrow C_2H_6O_2 + CO_2 / C_2H_6O_2 \rightarrow C_2H_4O_2 +$ $2H^+/PF_6^- + H^+ \rightarrow PF_5 + HF$, [63] respectively. Hence, moisture elimination in the battery is quite significant to suppress the production of POF₃. Lithium Bis(oxalato)borate (LiBOB) has attracted much attention due to its special properties, which can promote the SEI formation on both anodes and cathodes.^[65] However, LiBOB experiences a decomposition process at overcharge state and produces CO2 under the reaction with high active oxygen released from cathode material. The accumulated CO2 increases the battery internal pressure in a short time, which can break the "safety vent" and is regarded as a security assurance. [66] Vanchiappan and co-authors [67] present an overview on the properties of different kinds of lithium salts used in lithium batteries, which is an important reference for recognition and future selection of lithium salts.

Normally, electrolyte additives are selected to suppress gas evolution, which will be discussed in the following sections. However, they also contribute to more gas production during the electrochemical process. For instance, vinylene carbonate (VC) and vinyl ethylene carbonate (VEC) were noticed to evolve CO_2 and $\text{C}_4\text{H}_6\text{,}$ respectively (Figure 7e). $^{[61]}$ In 2014, Dahn's group^[68] studied the influence of electrolyte additives on battery gas evolution by monitoring the volume of the pouch cell using Archimedes' Principe, presenting that the combination of 2% VC and 2% Prop-1-ene 1,3-sultone (PES) successfully suppressed the gas evolution in graphite||NMC333 full cells. However, some additives, like Tris(trimethylsilyl) phosphite (TTSPi), contributed amounts of gas production. Hence, the selection of electrolyte additive is not arbitrary with monotonous regularity, but a choice based on the actual situation, where the cathode, anode, electrolyte solvent and salt applied are all needed to be considered for the best selection.

4.2. Solid (Semi-Solid) State Electrolyte

Solid-state electrolyte (SSE) is conducive to gas suppression which would be illustrated in the following section. However, solid-state electrolyte also faces the possibility of being disintegrated and produces gases.[16a,b,69] Torsten and co-authors[16a] studied the gas evolution of SSE batteries based on Ni-rich layered cathode (NCM622), and captured SO2 gas besides the traditional CO2 and O2 gases (Figure 8a,b). The produced gases were attributed to the decomposition of lithium thiophosphatebased SSE (β-Li₃PS₄) under the chemical reaction with highactive oxygen generated from the cathode. The evolution of SO₂ gas is highly depended on the electrolyte type^[16a] and the adopted anodes. [16b] As shown in Figure 8b, SO2 generation happens in β -Li₃PS₄ based cells but not in Li₆PS₅Cl based cells. As to the influence of anode selection on gas production of SSEs, researchers found that Li₄Ti₅O₁₂/Li₇Ti₅O₁₂ anode has the ability to suppress SO₂ evolution, where no SO₂ was captured, but not for Indium anode. Torsten's group also studied the affection of coating technique on gas suppression in solid-state batteries. [69] They prepared Li₂CO₃-coated and Li₂CO₃/LiNbO₃coated NCM622 cathodes that were tested in β -Li₃PS₄ based electrolyte (Figure 8c), finding that the gas evolution content was highly suppressed including CO₂, O₂, and SO₂ (Figure 8d). Above systemic studies show that solid-state batteries may be not the guarantee for next generation high energy density and high safety lithium batteries with no gas evolution, [1g] however, such optimization strategies are truly recommended which has been proved to work well.

Polymer electrolytes present good fire-resistant properties, poor liquidity and large mechanical strength, which are expected to be a good choice to improve the electrochemical performance and safety issues of lithium batteries. Polymer electrolytes suffer from low ionic conductivity and poor connection to electrodes, but can suppress the interface reaction between electrolyte and electrolyte as well as gas production.^[58a,70] Polymers electrolytes are not stable at high operating voltage and the associated gas release needs to pay more attention, like poly(ethylene oxide) (PEO). Kaihui and coauthors [71] tested the gas release of PEO under different voltages to 4.5 V, and various types of gases were detected, including H₂, CH₄, H₂O, C₂H₂, C₂H₄, CO, C₂H₆, HCHO, O₂, CH₃OH, CO₂, CH₃CHO, CH₃CH₂OH, and HCOOH. (Figure 8e) To clarify the gas evolution mechanism of PEO, the authors proposed a detailed decomposition process, revealing that the surface catalytic effect of LiCoO₂ on PEO is the root cause. As to the H₂ gas evolution in LiCoO₂|PEO-LiTFSI|Li solid polymer batteries, the oxidation/dehydration of PEO at the cathode side is more likely to produce H⁺, leading to the formation of strong acid HTFSI, which diffuses to the anode side and reacts with Li-metal to release H₂. The above-proposed process was proved by the density functional theory (DFT) calculations that H₂is very likely to originate from a crossover process of hydrated TFSI anions (HTFSI). (Figure 8f) For other kinds of polymers or oligomers, the study on gas evolution is limited, so more efforts need to be contributed for its safe and extensive applications.

Gas evolution detection and mechanism discussion for solid (semi-solid) state lithium batteries are rarely reported nowadays, which provides us more space to explore. SSE is regarded as the solution to fix the safety issue and the energy density limitation of lithium battery, but it also produces gas. Hence, it's imperative to study the relationship of gas production and performance decay in such battery systems, and clarify the corresponding mechanism for gas suppression.

5. Methods to Suppress Gas Generation

5.1. Buffer Layer Building between Material and Electrolyte

Gases generation is typically induced by the interfacial reactions between electrode materials and electrolytes, so avoiding the direct contact between the two parts seem to be the most feasible strategy. Normally, there are two ways to achieve it, which are electrode materials surface coating and solid electrolyte interface fabrication on both cathode and anode sides.

5.1.1. Coating Layer Construction

Surface coating seems to be the most obvious strategy, however, not all the substances can be used as coating medium, which

www.afm-journal.de

16163028, 2022, 47, Downloaded from https://adv

anced.onlinelibrary.wiley.com/doi/10.1002/adfm.202208586 by University Town Of Shenzhen, Wiley Online Library on [23/11/2025]. See the Terms

on Wiley Online Library for rules of use; OA articles are governed by the applicable Creative Commons License

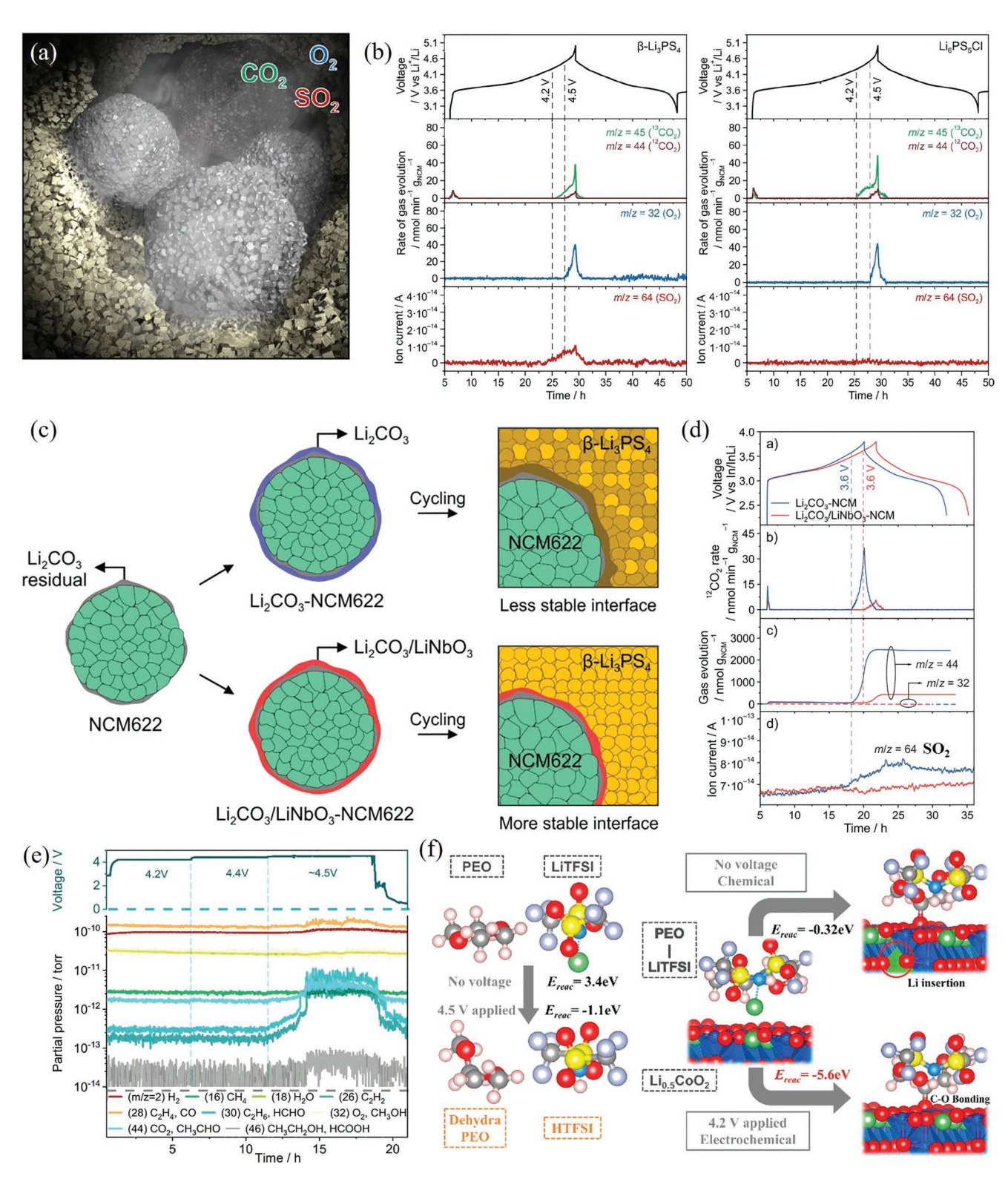


Figure 8. a) Distribution of electrode material and electrolyte in solid-state electrolyte. Reproduced with permission. [16al Copyright 2020, American Chemical Society. b) Voltage profiles of solid-state batteries using Li₃PS₄ and Li₆PS₅Cl solid electrolyte and corresponding in situ gas evolution rates of 12 CO₂, 13 CO₂, and SO₂. Reproduced with permission. [16al Copyright 2020, American Chemical Society. c) Illustration of the coating layer construction on the surface of NCM622 and the different interfacial reactivities when coupled with different coating substances. Reproduced with permission. [69l Copyright 2019, American Chemical Society. d) First cycle electrochemical curves of Li₂CO₃-coated and Li₂CO₃/LiNbO₃-coated NCM622 cathodes and the corresponding gas evolution processes. Reproduced with permission. [69l Copyright 2019, American Chemical Society. e) Voltage profiles and the corresponding gas evolution curves detected by DEMS. Reproduced with permission. [79l Copyright 2020, American Chemical Society. f) Theoretical calculations of reaction energies of PEO electrochemical oxidation on carbon electrode and LiCoO₂ electrode at 4.5 and 4.2 V, respectively. Reproduced with permission. [79l Copyright 2020, American Chemical Society.

16163028, 2022, 47, Downloaded from https://advanced.onlinelibrary.wiley.com/doi/10.1002/adfm.202208586 by University Town Of Shenzhen, Wiley Online Library on [23/11/2025]. See the Terms and Conditions

conditions) on Wiley Online Library for rules of use; OA articles are governed by the applicable Creative Commons

should meet the following requirements, including stable structure to electrolyte,[72] ionic conductor,[73] and capacity donor if possible. [74] Oxides and fluorides, [72a,75] including SiO₂, Al₂O₃, TiO₂, AlF₃, and FeF₃ et al., are typical coating materials with high structural stability and have been applied to passivate interfacial activity and improve the cycle stability. Inorganic lithium compound as fast ion conductor was always adopted as coating substance to forbidden the interfacial reaction and gas evolution during electrochemical process, like inorganic solid-state electrolytes, [73b,76] Li₃PO₄, [73a] LiTiO₂, [77] et al. Battery materials as coating substance present great values, which can not only protect the target materials, but also offer certain content of capacity. For example, Hu et al.[74a] prepared single crystal NMC622 coated with LiFePO4@C, which successfully suppressed the oxygen release of the delithiated NCM622 during heating. (Figure 9a-c) The improved performance was attributed to the strong absorption between PO₄³⁻ and transition metals, leading to the stabilization of the transition metal ions and oxygen ions on the surface against electrolyte. Similar method was applied on Li-rich layered cathode, by which the surface variation of crystal structure and TM ions migration are effectively restrained, resulting in an improved long-term cycling stability.^[74c] As to layered cathodes, including layered oxides and Li-rich layered cathodes, the main role of the coating layer should be able to suppress oxygen activity and eliminate the side reaction between electrode material and electrolyte.

However, surface coating layer cannot fully eliminate the oxygen release, thus suppressing the continuous oxygen loss remains a significant challenge.

As to anode, carbon coating is frequently adopted, which can not only suppress the gas evolution, but also can enhance conductivity and rate performance.^[78] He et al.^[38] constructed a carbon layer on the surface of LTO, which controlled the interfacial reactions between LTO and the surrounding electrolyte solution, and suppressed the gassing. Furthermore, the coated carbon is helpful for the SEI formation on LTO surface, which offers a significant synergy to separate LTO and electrolyte, preventing the interfacial gas evolution. Schiele et al.^[79] prepared core-shell structure of Si/C composite particles, which demonstrated positive effects on suppressing the issues faced by high-content Si anodes, including serious gassing behavior, bulk volume expansion, and mechanical degradation. (Figure 9d) As mentioned ahead, the main contribution of carbon coating layer in suppressing gas evolution to Si anode is to promote the formation of stable SEI layer and maintain the structure by weakening the volume expansion. Besides carbon coating, other forms of coating were also frequently applied, such as ceramic coating,[50,80] atomic layer deposition coating,^[81] multi-layer coating^[82] et al. For example, Lin and coauthors[81b] monitored the volatile species generated from the reaction between Li-metal and organic electrolytes, and found that the thin ALD protection layer on the Li-metal surface can

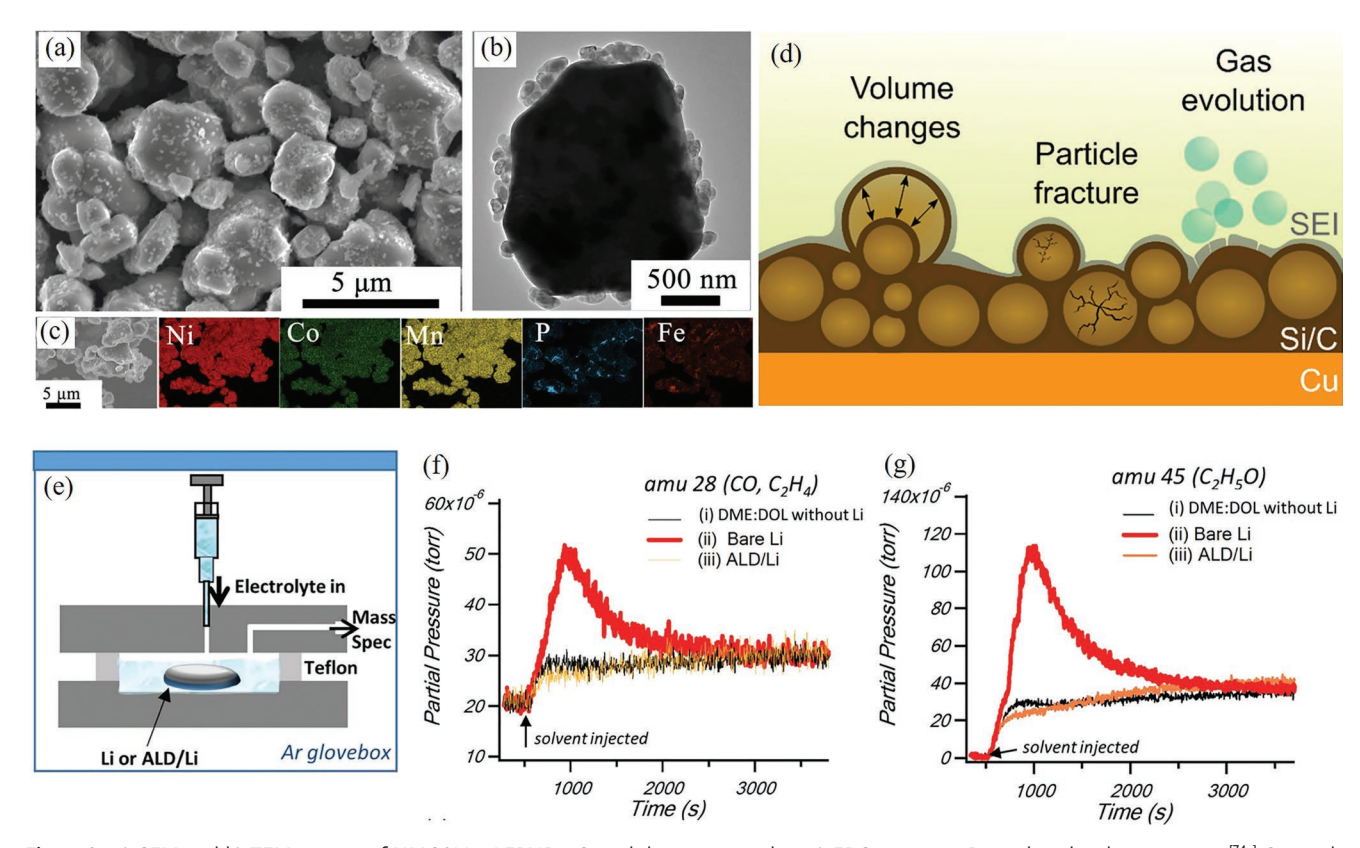


Figure 9. a) SEM and b) TEM images of NMC622@LFPNP@C, and the corresponding c) EDS mapping. Reproduced with permission. [74a] Copyright 2022, Elsevier. d) Schematic of polymer-derived carbon-coated silicon nanoparticles. Reproduced with permission. [79] Copyright 2022, American Chemical Society. Schematics of gas detection cell assembled in e) Ar-filled glovebox, f) m/z = 28, and g) m/z = 45 gas evolution data collected in DME/DOL without Li, DME/DOL with bare Li and DME/DOL with ALD coated Li@Al₂O₃. Reproduced with permission. [81b] Copyright 2016, John Wiley & Sons.

www.afm-journal.de

effectively forbidden the parasitic reaction and suppress the gas evolution (Figure 9e–g). The built ALD layer makes the Li-metal surface smooth and protects against the reaction between localized surface topographic features (like ridges and sharp edges) and electrolytes, resulting in the improvements of chemical and electrochemical stability of Li-metal anode. However, in different electrochemical conditions, the coating thickness should be optimized for better performances, which is not only for Li-metal anode, but also for other anode materials.

5.1.2. SEI Layer Construction

Electrolyte is a main component in lithium-ion batteries, which experiences side reaction with electrodes and forms by-products which covered on the electrode surface, leading to performance attenuation. Hence, high-quality electrolyte optimization is very important, which is conducive to the stable SEI formation on both cathode and anode to suppress parasitic reactions and solve gas production issues.^[58b]

Organic solvents, Li salts and electrolyte additives are the three main components of the liquid organic electrolyte. Organic solvents are the main contributor to the gas evolution by the reaction with electrode materials, such as EC, [1c,2b,22,36a,83] which is so important to the battery performance that we can't completely replace it with other solvents. Kasnatscheew and coauthors^[84] claimed that the EC-free electrolytes can promote the decomposition of LiPF₆ species and suppress the dissolution of transition metals, resulting in a superior electrochemical performance under high voltage conditions. However, its commercial value needsto further discuss. Goers et al.[85] successfully inhibited the gas evolution of Graphite||LiMn2O4 cells by applying ybutyrolactone (GBL) in EC-based liquid electrolyte (1:1 in weight). GBL as a co-solvent in carbonate electrolytes did a great job on gas suppression in graphite-based lithium batteries, which is much easier to be decomposed into stable SEI protective layer than EC.[86] As to Li salts, LiTFSI[51] or LiBF₄[87] was applied to replace LiPF₆, and found that the gas production was significantly suppressed. Recently, researchers found that bis(fluorosulfonyl)imide (FSI-) anion can promote the formation of robust SEI layer on Li metal anode, achieving high chemical stability for Li-based electric storage devices.^[88] Compared to LiTFSI, LiFSI is beneficial to protecting Al current collector from electrolytic corrosion.^[89] The credits of lithium fluoroalkylborate (LiFAB) can't be ignored, which functions better than LiPF₆- and LiBF₄-based electrolytes when coupled with graphite anode. Moreover, it demonstrates perfect endurance in the environment containing HF contamination relative to $LiPF_6$ and $LiBF_4$. [67,90] Dual-salt electrolytes were also widely applied to improve electrochemical performance and suppress the parasitic reaction between electrode materials and electrolytes, and the well-known combinations include lithium difluoro(oxalato)borate (LiDFOB)/LiBF₄,^[12a] LiPF₆/LiBF₄,^[87] spiro(1,1')-bipyrrolidinium tetrafluoroborate (SBPBF₄)/LiBF₄,^[91] LiTFSI/LiDFOB, [92] lithium trifluoro(perfluoro-tert-butyloxyl) borate (LiTFPFB)/LiTFSI,[93] et al. Additive occupies only a small amount to other components, but makes great contribution on forming protective layer on the electrode surface, which enables the separation of electrode materials and the

surrounding electrolyte to suppress the irreversible electrolyte decomposition. [58b,94] Plenty of literatures have done on additives and demonstrated excellent effects on gas suppression of electrolytes. [78,95] For example, Dahn and co-authors [95c,d] carried out series works to optimize the additive combination to suppress gas evolution and found that VC and lithium difluorophosphate are the very promising additives(Figure 10). Wu et al. [96] successfully suppressed the gassing behavior in TiNb2O7||LiFePO4 full cells by building a stable SEI on the anode surface with VC additive in electrolyte, which is helpful for preventing the continuous formation and dissolution of SEI film. The additives applied to modify SEI should be reduced (anode additives, low lowest unoccupied molecular orbital (LUMO)) or oxidized (cathode additives, high highest occupied molecular orbital (HOMO)) prior to other electrolyte components and prevent further decomposition of the SEI. Owing to the complex battery environment, muti-additive combination is recommended to be used to passive the electrode surface and suppress gas evolution effectively.

5.2. Material Structure Stabilization

Apart from the aforementioned buffer layer construction strategies on electrode materials, other methods including material doping,[97] surface modification,[98] morphology control[1c,99] and material design[100] are also applied to suppress the electrode activity and eliminate the parasitic reaction between active material and electrolyte. Doping method is the most frequentway to stable material structure by forming strong bonding between dopants and material elements. For example, Jung and coauthors[97a] synthesized boron-doped NMC cathode, which successfully improved cycle stability and suppressed gas evolution at high voltage. Moreover, by the comparison with phosphorous-doped NMC cathode, the author claimed that building oxygen stable facets is very important to suppress gas evolution and helpful for realizing state-of-the-art NMC cathodes. As shown in Figure 11a, both boron- and phosphorous-doped NMC cathodes demonstrated the textured microstructure, which is beneficial to suppressing the formation of microcracks, however, they presented different gas generation results owing to the different crystal faces for the two doped materials. Artificial surface modification was often adopted on Li-rich layered cathodes to suppress the surface oxygen activity. Meng and co-authors[98a] created a thin and uniform oxygen vacancy layer on the surface of Li-rich layered oxides by a gas-solid interface reaction method, which significantly suppressed gas release from the surface, including O2 and CO2. As explained, compared to the untreated sample, the oxygen vacancies introduced on the surface can hinder the generation of highly reactive oxygen radicals during the electrochemical process (Figure 11b). Coincidentally, Ramakrishnan and co-authors[98b] also applied "reactive" surface passivation techniques on Li-rich layered cathode to improve electrochemical performance and suppress gas production. Hu and co-authors[1c] did a representative work to illustrate the importance of morphology control on gas suppression that they synthesized polycrystalline and single crystal LiNi_{0.76}Mn_{0.14}Co_{0.1}O₂ (NMC76) cathodes (Figure 11c,d) and compared their gas evolution results. They found that the gas

www.afm-journal.de

16163028, 2022, 47, Downloaded from https://advanced.onlinelibrary.wiley.com/doi/10.1002/adfm.202208586 by University Town Of Shenzhen, Wiley Online Library on [23/11/2025]. See the Terms and Conditions (https://onlinelibrary.wiley.com/

and-conditions) on Wiley Online Library for rules of use; OA articles are governed by the applicable Creative Commons License

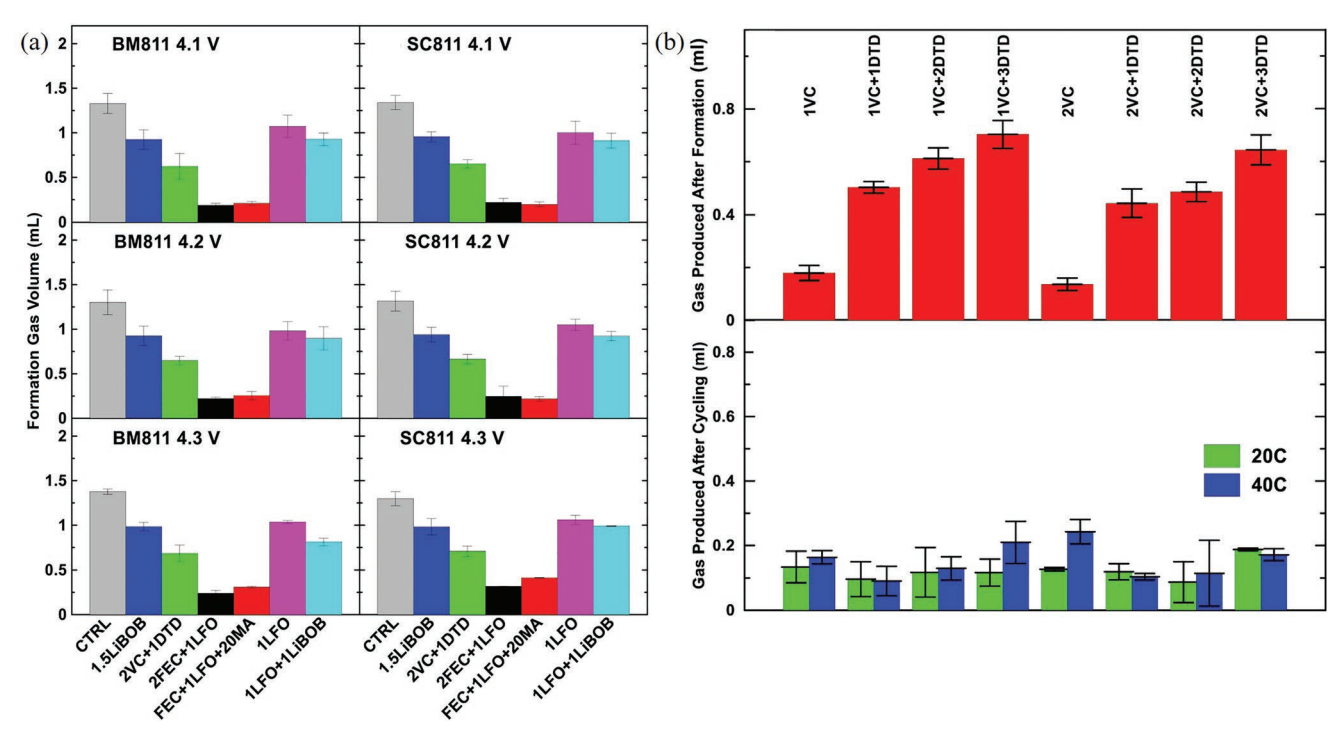


Figure 10. a) Gas evolution content comparison of NMC cathodes tested in carbonated electrolytes with different additives. Reproduced with permission. [95c] Copyright 2021, Electrochemical Society. b) Average gas evolution volume after formation cycle and long-term cycle tested with different additives. Reproduced with permission. [95d] Copyright 2021, Electrochemical Society.

evolution onsets and content of single crystal NMC cathode are less than those of polycrystalline cathode (Figure 11e,f), which can be attributed to the difference in morphology and surface area. Furthermore, material design is another option for the material stabilization, such as prelithiation technique. Xu et al.^[100b] made Li_xSn foil by Sn anode prelithiation, which presents a lower initial anode potential and promotes the formation of an adherent passivating SEI on the surface to suppress gas production. Without the prelithiation process, an isolated gas layer will be formed on the surface of Sn anode to cut off Li⁺ transport, leading to increased internal resistance and poor electrochemical performance.

5.3. Other Methods

Electrode components optimization and test conditions (e.g., temperature, voltage, and current density) are also significant in suppressing gas production during electrochemical operation. For instance, Hubert and co-authors^[32] presented a comprehensive study on anodic oxidation of conductive carbon in high-voltage Li-ion batteries, and found that conductive carbon (Super C65) was oxidized to CO/CO₂ when the cutoff voltage was set higher than 5.0 V. The gas evolution phenomenon was enhanced by the presence of water or high-temperature environment, as shown in **Figure 12**a. It is also revealed that the contribution of temperature on gas generation from electrolyte is larger than that from conductive carbon. For the study of H₂ originating from battery, Hubert et al.^[2b] developed an aluminum edge-seal diffusion barrier to elucidate separately the detailed reaction process of cathode and anode, demon-

strating H₂ evolution from H₂O reduction at graphite electrode is an important contributor (Figure 12b). Accordingly, for high loading electrode preparation, conductive carbon and residual water content should be carefully controlled to achieve high energy density and high safety lithium batteries. As to electrode binder, like Polyvinylidene Fluoride (PVDF), there is no gas evolution from itself up to 5.0 V, however, some binder can suppress battery gas production. For example, Buqa et al.[101] applied a water-based fluorine acrylic hybrid latex binder in LTO cells, which inhibited gas production by stabilizing the electrolyte. Battery voltage interval selection affects the state-of-charge (SOC) on both cathode and anode sides. Normally, at high SOC condition, the corresponding electrochemical activity will be highly enhanced, including oxidation ability of cathode and reduction ability of anode, resulting in serious parasitic interfacial reactions and plenty of gas production. [3a] By adjusting voltage window, battery gas evolution can be highly suppressed. For example, Ulriika and co-authors^[102] developed a functional electrochemical insitu mass spectrometry cell for gas evolution study of commercial cylindrical cells, and found that the CO₂ and H₂ generation content increased fast when the cutoff voltage is higher than 4.15 V or lower than 2.8 V. (Figure 12c) Moreover, C-rate dependency of gas evolution was noticed, like C₂H₄, which increased fast with the variation of C-rates from 1 to 4 C. Kozonoetal and co-authors[103] demonstrated that lowering the discharge voltage below 0.4 V is conducive to stabling SEI coating layer on LTO anode, resulting in efficient suppression on gas generation.

Electrolyte structure design was frequently applied to suppress gas evolution by restraining interfacial reaction, including high concentration electrolyte (HCE),[104] localized high concentration

16163028, 2022, 47, Downloaded from https://advanced.onlinelibrary.wiley.com/doi/10.1002/adfm.202208586 by University Town Of Shenzhen, Wiley Online Library on [23/11/2025]. See the Terms

md-conditions) on Wiley Online Library for rules of use; OA articles are governed by the applicable Creative Commons License

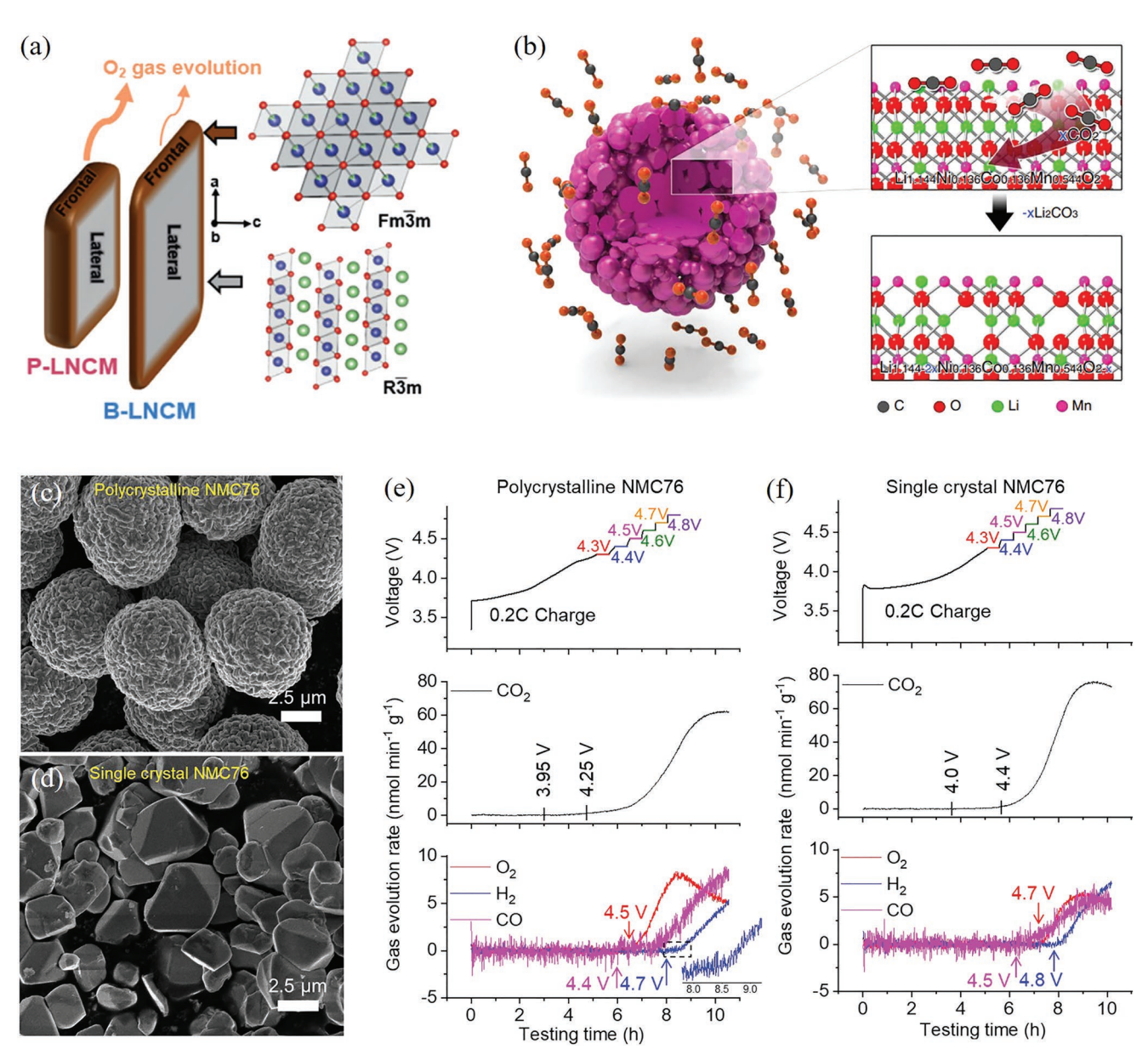


Figure 11. a) Schematic illustration of oxygen evolution from boron- and phosphorous-doped NMC cathodes. Reproduced with permission. [97a] Copyright 2021, John Wiley & Sons. b) Schematic demonstration of the gas solid interface reaction. Reproduced with permission. [98a] Copyright 2016, Springer Nature. c,d) SEM images of polycrystalline and single crystal NMC76. Reproduced with permission. [1c] Copyright 2022, Elsevier. e,f) The comparison of gas evolution onsets and contents between polycrystalline and single crystal NMC76 during the potential stepping procedures. Reproduced with permission. [1c] Copyright 2022, Elsevier.

electrolyte (LHCE),^[73c] solid-state electrolyte (SSE),^[16a,105] polymer electrolyte,^[70,106] ionic liquid electrolytes,^[107] et al. HCE is a typical example, where the labile solvents are bonded with cation-ions, achieving wider electrochemical stability window and suppressing gas production. Tong et al.^[104b] developed a concentrated electrolyte consisting of 4 M LiFSI in tetramethylene sulfone (TMS), which enabled a high working potential ≈6.0 V and dramatically suppressed gas formation during high voltage test in dual-ion batteries. In the concentrated LiFSI/TMS solution, the reduction of TES solvent at Li-metal anode was alleviated and the decomposition of LiFSI was promoted, which enhanced the formation of an F and N-rich SEI layer,

resulting in an improved electrochemical performance. In consideration of the high viscosity of HCEs, a new type of electrolyte was proposed, named as LHCE, [108] which can not only keep the strengths of HCE, but also can improve the lithium diffusion ability. The main strategy of this electrolyte is to choose an "inert" diluent that does not dissolve the salt but is miscible with the solvent applied. Especially, in Li-metal batteries, LHCE can successfully suppress the interfacial parasitic reaction with Li-metal, resulting in improved electrochemical performance and limited side products. [109] Moreover, the concept of "waterin-salt" (Figure 12d) applied in aqueous electrolytes also aims to decrease the activity of water molecules and improve its

www.afm-journal.de

16163028, 2022, 47, Downloaded from https://adv

anced.onlinelibrary.wiley.com/doi/10.1002/adfm.202208586 by University Town Of Shenzhen, Wiley Online Library on [23/11/2025]. See the Terms

inditions) on Wiley Online Library for rules of use; OA articles are governed by the applicable Creative Commons

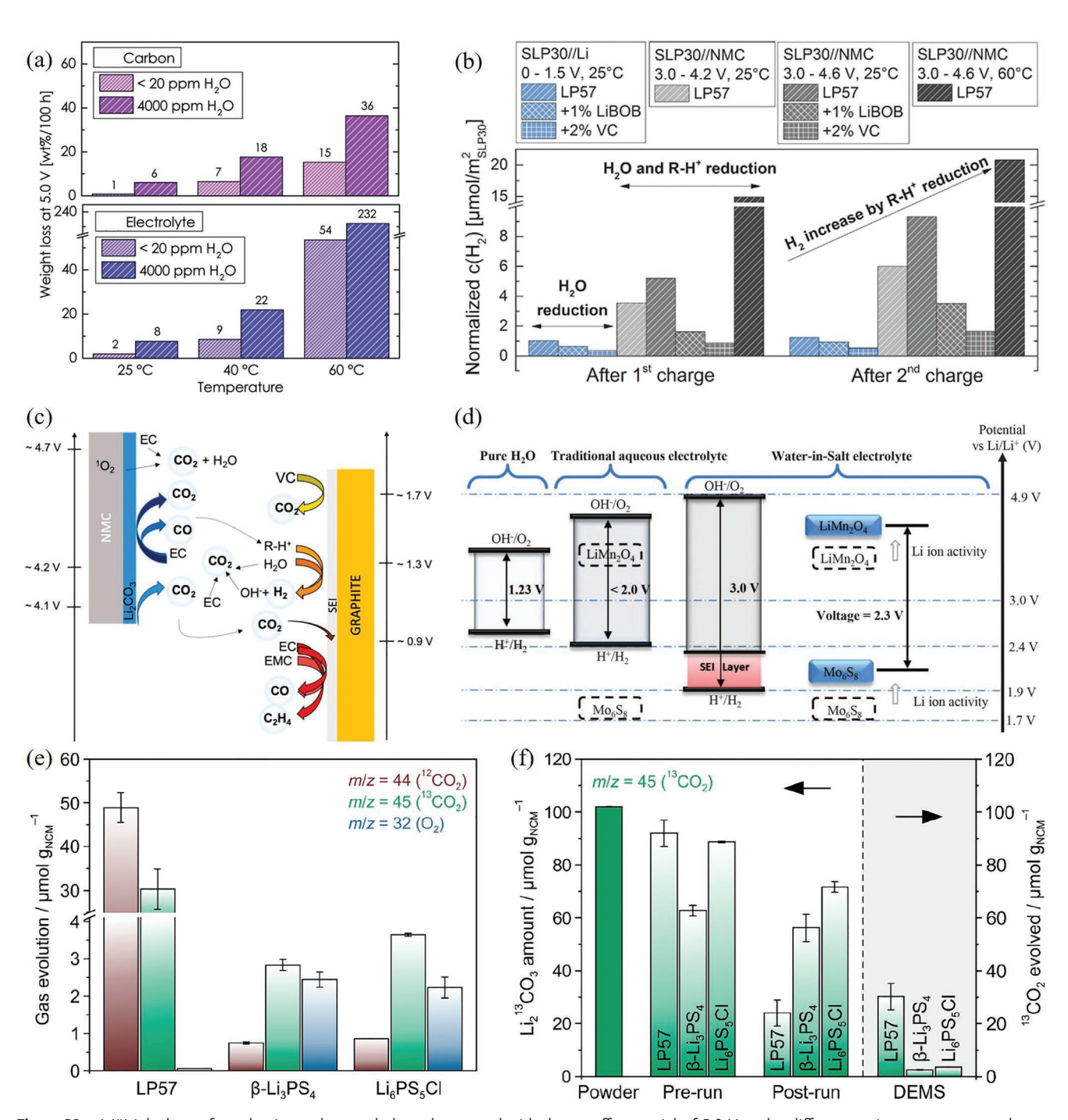


Figure 12. a) Weight loss of conductive carbon and electrolyte tested with the cutoff potential of 5.0 V under different moisture contents and temperatures. Reproduced with permission. (32) Copyright 2015, Elsevier. b) H_2 concentrations of SLP||Li after 1st and 2nd charge tested in different cell configurations and different electrolytes. Reproduced with permission. (2b) Copyright 2016, Elsevier. c) Schematic of the commonly observed gases under different voltages, including CO_2 , CO, C_2H_4 , and CO0. Reproduced with permission. (102) Copyright 2010, Elsevier. e,f) Gas evolution comparison between LP57, CO1. CO1. CO2 And CO3. Reproduced with permission. (104) Copyright 2010, Elsevier. e,f) Gas evolution comparison between LP57, CO3. And CO4. Copyright 2020, American Chemical Society.

stability during electrochemical process, which captured much researchers' attention in the last ten years.^[110] As to other kinds of electrolyte structure, adhering the same concept to HCE, they were selected to decrease the possibility of adverse side reactions by means of their merits. For instance, Torsten and

co-authors^[16a] first compared gas evolution in different electrolyte systems based on Ni-rich layered cathodes, including SSE (β -Li₃PS₄ and Li₆PS₅Cl) and liquid electrolytes (LP57, 1 \upmu LiPF₆ in 3:7 by weight EC and EMC), and proved that the cumulative amount of gases released from liquid electrolyte based lithium

www.afm-journal.de

16163028, 2022, 47, Downloaded from https://advanced.onlinelibrary.wiley.com/doi/10.1002/adfm.202208886 by University Town Of Shenzhen, Wiley Online Library on [23/11/2025]. See the Terms and Conditions (https://onlinelibrary.wiley

conditions) on Wiley Online Library for rules of use; OA articles are governed by the applicable Creative Commons License

batteries is higher than that in SSB cells. (Figure 12e,f) Li and co-authors^[70] developed a dual-functional gel-polymer electrolyte, which greatly suppressed the gas production, especially for the graphite-Si/C anode batteries. The gel-polymer based batteries did not experience violent combustion during needle penetration test.

6. Conclusion and Perspective

In the last decades, gas generation in lithium battery hasreceived more and more attention due to its great influence on battery development and commercial applications. Here, we first reviewed the gas evolution mechanismsof cathode materials, anode materials and electrolytes, which enable us a comprehensive and unified understanding of the gas production situation from the common battery system. The gas evolution prevention strategies were also summarized, including buffer layer construction between electrode materials and electrolytes, electrode materials optimization and modification, electrode components and electrolyte structure design, test condition adjustment, et al., which can open the horizon for gas prevention and is expected to provide reference for more efficient gas suppression strategies. It's not easy to suppress gas completely just based on one or two strategies, because the gases observedfrom battery may originate from different components, including cathode, anode, electrolyte, conductive carbon, residue water, et al. It is a kind of enormous project for radical gas evolution suppression that every part of the battery should be paid special attention to. It is of great significant to suppress gas toachieve high electrochemical performance and high safety for the future high energy density lithium batteries.

Gas detection and analysis are the basis to solve gas evolution issue in lithium battery. However, the most frequently adopted equipment, namely DEMS, has great limitations, such as limited gas detection duration induced by the electrolyte evaporation, deviation from real battery system owing to the use of large amount of electrolyte, accuracy of the collected gas production

results, et al., hence measurements for further improvement of DEMS is necessary and important. With the convincing gas production results, the gas evolution mechanism can be concluded in a precise way, which is not only rewarding for the analysis of the root attenuation reason of battery, but also for providing precise and targeted strategies for gas suppression. Combining the above review with the gas detecting deficiencies, a short perspective for future gas evolution analysis and suppression is proposed as follows (Figure 13):

- 1) Long-term gas test ability with high precision. A multi-functional in situ DEMS equipment is expected to be designed and developed, which should enable the following requests, including long-term test duration, advancedvolatile electrolyte condensation and replenishment system, high sensitivity for gas detection, a standard and repeatable gas testing protocol, et al. In commercial battery testing, flatulent phenomenon always appears after hundreds of cycles, which is far beyond the ability of DEMS. Hence, a long-term testing ability is needed, capable of affording an in situ gas evolution analysis during the long-term cycling. Part of the electrolyte can be carried away by the vacuum system or carrier gas, which will shorten battery life and blockthe capillary tube to affect the equipment sensitivity. Thus the condensation system is needed to trap the evaporable electrolyte and then reduce the interference to instrument sensitivity and test results. Furthermore, in the long-term study of gas generation in lithium batteries, internal gas consumption needs to be considered for an accurate analysis. Normally, gas content produced from DEMS cell is limited, and the corresponding quantified result from different batches is difficult to repeat, hence a universal testing protocol is very important and deserved to be promoted, which has been proved by Jie and co-authors.^[1c]
- 2) Scientificdesign ofgas testing process. Scientific discussion of gas production mechanism is crucial to reveal the liuthium battery attenuation process, which can fundamentally clarify the internalcomplex chemical reactions when coupled with other high-resolution characterizations. Considering

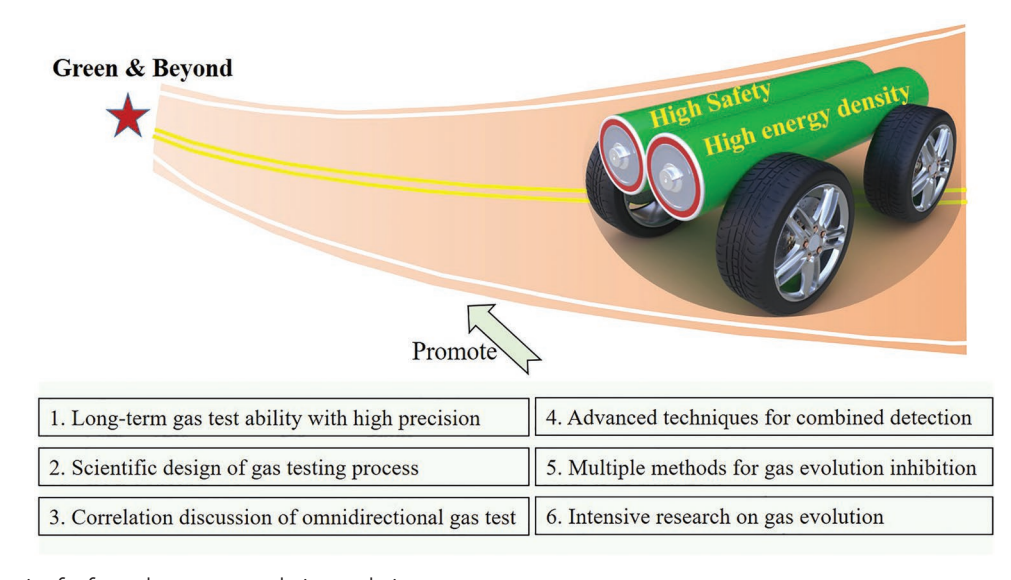


Figure 13. Perspective for future battery gas evolution analysis.





www.afm-journal.de

its complexity caused by cross-talk reactions, the separate studies (namely the half-cell) of the applied cathode and anode are recommended, where LiFePO₄ can be used and regarded as an important reference. Thereafter, full-cell gas evolution investigation is suggested to follow up for the analysis of cross-talk reactions by studying the gas categories and contents.

- 3) Correlation discussion of omnidirectional gas test. Systematic studies on gassingshould be done under normal work condition and thermal runaway situation (high temperature, overcharge, short circuits, et al.), which is conducive to building the correlation between the two gas evolution mechanisms. By analyzing the internal correlation, more effective measurement for gas generation suppression can be precisely proposed to solve the issues of gas generation and battery safety. Up to now, most studies have focused onthese two conditions separately, which is not conducive to a comprehensive understanding of the battery gas evolution processes. So it is of great significant to establish the correlation mechanism of gas production under the two backgrounds.
- 4) Advanced techniques for combined detection. More efforts on developing precise techniques for detection are needed. They are designed to offset each technique's limitation to maximize the gas information for better understanding of gas evolution mechanism. In situ DEMS provides the information of gas evolution onsets and gas contents, which can be coupled with other techniques to probe solid and liquid reaction products to estimate the gas evolution mechanism, such as in situ high resolution transmission electron microscopy, and nuclear magnetic resonance spectroscopy, respectively.
- 5) Multiple methods for gas evolution inhibition. There are many gas sources generated in the battery, so all the possible components for gas generation should be modified and optimized before battery assembly. The reviewed gas suppression methods, including buffer layer construction, electrolyte optimization, testing condition selection, et al., are not the state-of-the-art techniques, which need further modification. For instance, the extent of the coating's coverage on the electrode surface is often nonuniform, [111] resulting in the continuous interfacial parasitic reactions and gas production. Hence, it requires the simultaneous implementation of multiple measures to suppress gases. On the other hand, multiple suppression measures are also necessary. For example, singlet oxygen released from NMC cathodes is the fuse of gas evolution, and the most direct way is to lock the surface oxygen. Element doping is regarded as an efficient way, however, it is impossible to fully solve the gas issue. Hence, coating layer construction together with electrolyte screening may be necessary and recommended to participate in gas evolution inhibition.
- 6) Intensive researchon gas evolution. Mechanism analysis and suppression methods of gas evolution on normal condition and thermal runaway circumstance can restrain the complex battery safety issue, and improve the electrochemical performancesimultaneously. That is because the gas suppression methods are normally chosen to stable the electrode materials and electrolyte, which are the main determinants for battery performance. Hence, gas analysis is definitely an efficient and valuable technology in achieving high safety and

high electrochemical performance lithium batteries.Intensive research on gas evolution is deserved to get more attention for practical battery application.

Acknowledgements

This work was funded by the National Key Research and Development Program of China (No. 2020YFC1909604), National Natural Science Foundation of China (No. 52002248), Shenzhen Basic Research Program (No. JCYJ20190808163005631).

Conflict of Interest

The authors declare no conflict of interest.

Keywords

gas generation, lithium batteries, performance decay, safer operations

Received: July 26, 2022 Revised: August 26, 2022 Published online: September 22, 2022 16163028, 2022, 47, Downloaded from https://advanced.onlinelibrary.wiley.com/doi/10.1002/adfm.202208586 by University Town Of Shenzhen, Wiley Online Library on [23/11/2025]. See the Terms and Conditions (https://onlinelibrary.wiley.com/terms

-and-conditions) on Wiley Online Library for rules of use; OA articles are governed by the applicable Creative Commons License

- [1] a) J. Duan, X. Tang, H. Dai, Y. Yang, W. Wu, X. Wei, Y. Huang, Electrochem. Energy Rev. 2019, 3, 1; b) K. Liu, Y. Liu, D. Lin, A. Pei, Y. Cui, Sci. Adv. 2018, 4, eaas9820; c) J. Hu, L. Li, Y. Bi, J. Tao, J. Lochala, D. Liu, B. Wu, X. Cao, S. Chae, C. Wang, J. Xiao, Energy Stor. Mater. 2022, 47, 195; d) L. Kong, C. Li, J. Jiang, M. Pecht, Energies 2018, 11, 2191; e) X. Feng, M. Ouyang, X. Liu, L. Lu, Y. Xia, X. He, Energy Stor. Mater. 2018, 10, 246; f) B. Rowden, N. Garcia-Araez, Energy Rep. 2020, 6, 10; g) A. M. Bates, Y. Preger, L. Torres-Castro, K. L. Harrison, S. J. Harris, J. Hewson, Joule 2022, 6, 742
- a) D. J. Xiong, R. Petibon, M. Nie, L. Ma, J. Xia, J. R. Dahn, J. Electrochem. Soc. 2016, 163, A546; b) M. Metzger, B. Strehle, S. Solchenbach, H. A. Gasteiger, J. Electrochem. Soc. 2016, 163, A798; c) D. J. Xiong, L. D. Ellis, R. Petibon, T. Hynes, Q. Q. Liu, J. R. Dahn, J. Electrochem. Soc. 2016, 164, A340; d) L. Ellis, J. R. Dahn, Meet. Abstr. 2016, 2, 236; e) S. E. Sloop, J. B. Kerr, K. Kinoshita, J. Power Sources 2003, 119, 330; f) D. J. Xiong, L. D. Ellis, K. J. Nelson, T. Hynes, R. Petibon, J. R. Dahn, J. Electrochem. Soc. 2016, 163, A3069.
- [3] a) J. Wandt, A. T. S. Freiberg, A. Ogrodnik, H. A. Gasteiger, *Mater. Today* 2018, 21, 825; b) M. Raghibi, B. Xiong, S. Phadke, M. Anouti, *Electrochim. Acta* 2020, 362, 137214.
- [4] a) X. Liu, D. Ren, H. Hsu, X. Feng, G.-L. Xu, M. Zhuang, H. Gao, L. Lu, X. Han, Z. Chu, J. Li, X. He, K. Amine, M. Ouyang, Joule 2018, 2, 2047; b) J. Liu, Z. Bao, Y. Cui, E. J. Dufek, J. B. Goodenough, P. Khalifah, Q. Li, B. Y. Liaw, P. Liu, A. Manthiram, Y. S. Meng, V. R. Subramanian, M. F. Toney, V. V. Viswanathan, M. S. Whittingham, J. Xiao, W. Xu, J. Yang, X.-Q. Yang, J.-G. Zhang, Nat. Energy 2019, 4, 180.
- [5] a) J. Zheng, S. Myeong, W. Cho, P. Yan, J. Xiao, C. Wang, J. Cho, J.-G. Zhang, Adv. Energy Mater. 2017, 7, 1601284; b) P. Rozier, J. M. Tarascon, J. Electrochem. Soc. 2015, 162, A2490.
- [6] a) M. Ko, S. Chae, J. Ma, N. Kim, H.-W. Lee, Y. Cui, J. Cho, Nat. Energy 2016, 1, 16113; b) S. Chae, Y. Xu, R. Yi, H.-S. Lim, D. Velickovic, X. Li, Q. Li, C. Wang, J.-G. Zhang, Adv. Mater. 2021, 33, 2103095.

16163028, 2022, 47, Downloaded from https://advanced.onlinelibrary.wiley.com/doi/10.1002/adfm.202208586 by University Town Of Shenzhen, Wiley Online Library on [23/11/2025]. See the Terms

and Conditions

conditions) on Wiley Online Library for rules of use; OA articles are governed by the applicable Creative Commons

www.advancedsciencenews.com www.afm-journal.de

- [7] a) C. Niu, H. Lee, S. Chen, Q. Li, J. Du, W. Xu, J.-G. Zhang, M. S. Whittingham, J. Xiao, J. Liu, Nat. Energy 2019, 4, 551;
 b) C. Niu, D. Liu, J. A. Lochala, C. S. Anderson, X. Cao, M. E. Gross, W. Xu, J.-G. Zhang, M. S. Whittingham, J. Xiao, J. Liu, Nat. Energy 2021, 6, 723.
- [8] a) X. Liu, L. Yin, D. Ren, L. Wang, Y. Ren, W. Xu, S. Lapidus, H. Wang, X. He, Z. Chen, G.-L. Xu, M. Ouyang, K. Amine, *Nat. Commun.* 2021, 12, 4235; b) D. Ren, X. Feng, L. Lu, M. Ouyang, S. Zheng, J. Li, X. He, *J. Power Sources* 2017, 364, 328.
- [9] a) C. P. Aiken, J. Self, R. Petibon, X. Xia, J. M. Paulsen, J. R. Dahn, J. Electrochem. Soc. 2015, 162, A760; b) D. Aurbach, J. Power Sources 2000, 89, 206.
- [10] Y. Zeng, K. Wu, D. Wang, Z. Wang, L. Chen, J. Power Sources 2006, 160, 1302.
- [11] D. P. Finegan, E. Darcy, M. Keyser, B. Tjaden, T. M. M. Heenan, R. Jervis, J. J. Bailey, N. T. Vo, O. V. Magdysyuk, M. Drakopoulos, M. Di Michiel, A. Rack, G. Hinds, D. J. L. Brett, P. R. Shearing, Adv. Sci. 2018, 5, 1870003.
- [12] a) A. J. Louli, A. Eldesoky, R. Weber, M. Genovese, M. Coon, J. deGooyer, Z. Deng, R. T. White, J. Lee, T. Rodgers, R. Petibon, S. Hy, S. J. H. Cheng, J. R. Dahn, Nat. Energy 2020, 5, 693; b) W.-t. Luo, S.-b. Zhu, J.-h. Gong, Z. Zhou, Procedia Eng 2018, 211, 531
- [13] F. Larsson, B.-E. Mellander, J. Electrochem. Soc. 2014, 161, A1611.
- [14] Q. Wang, P. Ping, X. Zhao, G. Chu, J. Sun, C. Chen, J. Power Sources 2012, 208, 210.
- [15] a) S.-M. Bak, E. Hu, Y. Zhou, X. Yu, S. D. Senanayake, S.-J. Cho, K.-B. Kim, K. Y. Chung, X.-Q. Yang, K.-W. Nam, ACS Appl. Mater. Interfaces 2014, 6, 22594; b) H.-J. Noh, S. Youn, C. S. Yoon, Y.-K. Sun, J. Power Sources 2013, 233, 121; c) Q. Xie, Z. Cui, A. Manthiram, Adv. Mater. 2021, 33, 2100804.
- [16] a) F. Strauss, J. H. Teo, A. Schiele, T. Bartsch, T. Hatsukade, P. Hartmann, J. Janek, T. Brezesinski, ACS Appl. Mater. Interfaces 2020, 12, 20462; b) T. Bartsch, F. Strauss, T. Hatsukade, A. Schiele, A. Y. Kim, P. Hartmann, J. Janek, T. Brezesinski, ACS Energy Lett. 2018, 3, 2539; c) A. A. Delluva, J. Kulberg-Savercool, A. Holewinski, Adv. Funct. Mater. 2021, 31, 2103716; d) R. Jung, M. Metzger, F. Maglia, C. Stinner, H. A. Gasteiger, J. Phys. Chem. Lett. 2017, 8, 4820.
- [17] a) B. Strehle, K. Kleiner, R. Jung, F. Chesneau, M. Mendez,
 H. A. Gasteiger, M. Piana, J. Electrochem. Soc. 2017, 164, A400;
 b) S. E. Renfrew, B. D. McCloskey, J. Am. Chem. Soc. 2017, 139, 17853
- [18] a) Y. Kim, H. Park, J. H. Warner, A. Manthiram, ACS Energy Lett. 2021, 6, 941; b) J. R. Dahn, E. W. Fuller, M. Obrovac, U. von Sacken, Solid State Ion 1994, 69, 265; c) K. Kim, H. Ma, S. Park, N.-S. Choi, ACS Energy Lett. 2020, 5, 1537.
- [19] N. Mahne, S. E. Renfrew, B. D. McCloskey, S. A. Freunberger, Angew. Chem., Int. Ed. 2018, 57, 5529.
- [20] T. Hatsukade, A. Schiele, P. Hartmann, T. Brezesinski, J. Janek, ACS Appl. Mater. Interfaces 2018, 10, 38892.
- [21] a) K. Kanamura, S. Toriyama, S. Shiraishi, Z. i. Takehara, J. Electrochem. Soc. 1995, 142, 1383; b) Y. Kim, J. Solid State Electrochem. 2013, 17, 1961.
- [22] R. Jung, M. Metzger, F. Maglia, C. Stinner, H. A. Gasteiger, J. Electrochem. Soc. 2017, 164, A1361.
- [23] J. Li, A. R. Cameron, H. Li, S. Glazier, D. Xiong, M. Chatzidakis, J. Allen, G. A. Botton, J. R. Dahn, J. Electrochem. Soc. 2017, 164, A1534.
- [24] a) K. Luo, M. R. Roberts, N. Guerrini, N. Tapia-Ruiz, R. Hao, F. Massel, D. M. Pickup, S. Ramos, Y.-S. Liu, J. Guo, A. V. Chadwick, L. C. Duda, P. G. Bruce, J. Am. Chem. Soc. 2016, 138, 11211; b) K. Luo, M. R. Roberts, R. Hao, N. Guerrini, D. M. Pickup, Y.-S. Liu, K. Edström, J. Guo, A. V. Chadwick, L. C. Duda, P. G. Bruce, Nat. Chem. 2016, 8, 684.

- [25] J. Rana, J. K. Papp, Z. Lebens-Higgins, M. Zuba, L. A. Kaufman, A. Goel, R. Schmuch, M. Winter, M. S. Whittingham, W. Yang, B. D. McCloskey, L. F. J. Piper, ACS Energy Lett. 2020, 5, 634.
- [26] H. Q. Pham, Ł. Kondracki, M. Tarik, S. Trabesinger, J. Power Sources 2022, 527, 231181.
- [27] S. Shen, Y. Hong, F. Zhu, Z. Cao, Y. Li, F. Ke, J. Fan, L. Zhou, L. Wu, P. Dai, M. Cai, L. Huang, Z. Zhou, J. Li, Q. Wu, S. Sun, ACS Appl. Mater. Interfaces 2018, 10, 12666.
- [28] T. M. Bandhauer, S. Garimella, T. F. Fuller, J. Electrochem. Soc. 2011, 158 R1
- [29] S.-M. Bak, K.-W. Nam, W. Chang, X. Yu, E. Hu, S. Hwang, E. A. Stach, K.-B. Kim, K. Y. Chung, X.-Q. Yang, Chem. Mater. 2013, 25, 337.
- [30] M. Guilmard, L. Croguennec, D. Denux, C. Delmas, Chem. Mater. 2003, 15, 4476.
- [31] A. Kajiyama, R. Masaki, T. Wakiyama, K. Matsumoto, A. Yoda, T. Inada, H. Yokota, R. Kanno, J. Electrochem. Soc. 2015, 162, A1516.
- [32] M. Metzger, C. Marino, J. Sicklinger, D. Haering, H. A. Gasteiger, J. Electrochem. Soc. 2015, 162, A1123.
- [33] M. Metzger, J. Sicklinger, D. Haering, C. Kavakli, C. Stinner, C. Marino, H. A. Gasteiger, J. Electrochem. Soc. 2015, 162, A1227.
- [34] M. Metzger, P. Walke, B. Strehle, S. Solchenbach, H. A. Gasteiger,
- Meet. Abstr. 2016, 2, 322.
 [35] R. Bernhard, M. Metzger, H. A. Gasteiger, J. Electrochem. Soc. 2015, 162, A1984.
- [36] a) G. Gachot, P. Ribière, D. Mathiron, S. Grugeon, M. Armand, J.-B. Leriche, S. Pilard, S. Laruelle, Anal. Chem. 2011, 83, 478; b) R. Petibon, L. M. Rotermund, J. R. Dahn, J. Power Sources 2015, 287, 184
- [37] R. Mogi, M. Inaba, Y. Iriyama, T. Abe, Z. Ogumi, J. Power Sources 2003. 597, 119.
- [38] Y.-B. He, B. Li, M. Liu, C. Zhang, W. Lv, C. Yang, J. Li, H. Du, B. Zhang, Q.-H. Yang, J.-K. Kim, F. Kang, Sci. Rep. 2012, 2, 913.
- [39] a) I. Belharouak, G. M. Koenig, K. Amine, J. Power Sources 2011, 196, 10344; b) I. Belharouak, G. M. Koenig, T. Tan, H. Yumoto, N. Ota, K. Amine, J. Electrochem. Soc. 2012, 159, A1165.
- [40] a) A. M. Andersson, K. Edström, N. Rao, Å. Wendsjö, J. Power Sources 1999, 81, 286; b) M. Holzapfel, F. Alloin, R. Yazami, Electrochim. Acta 2004, 49, 581.
- [41] K. Wu, J. Yang, Y. Zhang, C. Wang, D. Wang, J. Appl. Electrochem. 2012, 42, 989.
- [42] a) I. A. Profatilova, S.-S. Kim, N.-S. Choi, Electrochim. Acta 2009, 54, 4445; b) M.-H. Ryou, J.-N. Lee, D. J. Lee, W.-K. Kim, Y. K. Jeong, J. W. Choi, J.-K. Park, Y. M. Lee, Electrochim. Acta 2012, 83, 259; c) A. D. Pasquier, F. Disma, T. Bowmer, A. S. Gozdz, G. Amatucci, J. M. Tarascon, J. Electrochem. Soc. 1998, 145, 472.
- [43] H. Maleki, G. Deng, A. Anani, J. Howard, J. Electrochem. Soc. 1999, 146, 3224.
- [44] T. Yoon, M. S. Milien, B. S. Parimalam, B. L. Lucht, Chem. Mater. 2017, 29, 3237.
- [45] I. Watanabe, J.-i. Yamaki, J. Power Sources 2006, 153, 402.
- [46] K. Wu, J. Yang, Y. Liu, Y. Zhang, C. Wang, J. Xu, F. Ning, D. Wang, J. Power Sources 2013, 237, 285.
- [47] J.-i. Yamaki, H. Takatsuji, T. Kawamura, M. Egashira, Solid State Ion 2002, 148, 241.
- [48] E. Iwama, T. Ueda, Y. Ishihara, K. Ohshima, W. Naoi, M. T. H. Reid, K. Naoi, Electrochim. Acta 2019, 301, 312.
- [49] C. R. Fell, L. Sun, P. B. Hallac, B. Metz, B. Sisk, J. Electrochem. Soc. 2015, 162, A1916.
- [50] M. He, E. Castel, A. Laumann, G. Nuspl, P. Novák, E. J. Berg, J. Electrochem. Soc. 2015, 162, A870.
- [51] R. Bernhard, S. Meini, H. A. Gasteiger, J. Electrochem. Soc. 2014, 161. A497.
- [52] M. Metzger, B. Strehle, S. Solchenbach, H. A. Gasteiger, J. Electrochem. Soc. 2016, 163, A1219.

www.afm-journal.de

16163028, 2022, 47, Downloaded from https://advanced.onlinelibrary.

wiley.com/doi/10.1002/adfm.202208586 by University Town Of Shenzhen, Wiley Online Library on [23/11/2025]. See the Terms

and Conditions

of use; OA articles are governed by the applicable Creative Commons

- [53] J. C. Burns, A. Kassam, N. N. Sinha, L. E. Downie, L. Solnickova, B. M. Way, J. R. Dahn, J. Electrochem. Soc. 2013, 160, A1451.
- [54] U. Mattinen, M. Klett, G. Lindbergh, R. Wreland Lindström, J. Power Sources 2020, 477, 228968.
- [55] A. Wuersig, W. Scheifele, P. Novák, J. Electrochem. Soc. 2007, 154, A449.
- [56] L. D. Ellis, J. P. Allen, L. M. Thompson, J. E. Harlow, W. J. Stone, I. G. Hill, J. R. Dahn, J. Electrochem. Soc. 2017, 164, A3518.
- [57] B. Michalak, H. Sommer, D. Mannes, A. Kaestner, T. Brezesinski, J. Janek, Sci. Rep. 2015, 5, 15627.
- [58] a) K. Xu, Chem. Rev. 2014, 114, 11503; b) K. Xu, Chem. Rev. 2004, 104, 4303.
- [59] K. Xu, A. von Cresce, J. Mater Chem. 2011, 21, 9849.
- [60] H. Yang, G. V. Zhuang, P. N. Ross, J. Power Sources 2006, 161, 573.
- [61] B. Strehle, S. Solchenbach, M. Metzger, K. U. Schwenke, H. A. Gasteiger, J. Electrochem. Soc. 2017, 164, A2513.
- [62] J. Liu, P. Bian, J. Li, W. Ji, H. Hao, A. Yu, J. Power Sources 2015, 286,
- [63] M. Metzger, P. Walke, S. Solchenbach, G. Salitra, D. Aurbach, H. A. Gasteiger, J. Electrochem. Soc. 2020, 167, 160522.
- [64] D. Strmcnik, I. E. Castelli, J. G. Connell, D. Haering, M. Zorko, P. Martins, P. P. Lopes, B. Genorio, T. Østergaard, H. A. Gasteiger, F. Maglia, B. K. Antonopoulos, V. R. Stamenkovic, J. Rossmeisl, N. M. Markovic, Nat. Catal. 2018, 1, 255.
- [65] a) W. Xu, C. A. Angell, Electrochem. Solid-State Lett. 2001, 4, E1; b) W. Xu, C. A. Angell, Solid State Ion 2002, 147, 295.
- [66] S. Shui Zhang, Electrochem. Commun. 2006, 8, 1423.
- [67] V. Aravindan, J. Gnanaraj, S. Madhavi, H.-K. Liu, Chem. Eur. J. **2011**, *17*, 14326.
- [68] C. P. Aiken, J. Xia, D. Y. Wang, D. A. Stevens, S. Trussler, J. R. Dahn, J. Electrochem. Soc. 2014, 161, A1548.
- [69] A. Y. Kim, F. Strauss, T. Bartsch, J. H. Teo, T. Hatsukade, A. Mazilkin, J. Janek, P. Hartmann, T. Brezesinski, Chem. Mater. 2019. 31. 9664.
- [70] X. Li, K. Qian, Y.-B. He, C. Liu, D. An, Y. Li, D. Zhou, Z. Lin, B. Li, Q.-H. Yang, F. Kang, J. Mater. Chem. A 2017, 5, 18888.
- [71] K. Nie, X. Wang, J. Qiu, Y. Wang, Q. Yang, J. Xu, X. Yu, H. Li, X. Huang, L. Chen, ACS Energy Lett. 2020, 5, 826.
- [72] a) S.-H. Lee, G.-J. Park, S.-J. Sim, B.-S. Jin, H.-S. Kim, J. Alloys Compd. 2019, 791, 193; b) J. Li, L. Wang, Q. Zhang, X. He, J. Power Sources 2009, 190, 149.
- [73] a) P. Yan, J. Zheng, J. Liu, B. Wang, X. Cheng, Y. Zhang, X. Sun, C. Wang, J.-G. Zhang, Nat. Energy 2018, 3, 600; b) Y. Kim, Phys. Chem. Chem. Phys. 2013, 15, 6400; c) J.-M. Kim, Y. Xu, M. H. Engelhard, J. Hu, H.-S. Lim, H. Jia, Z. Yang, B. E. Matthews, S. Tripathi, X. Zhang, L. Zhong, F. Lin, C. Wang, W. Xu, ACS Appl. Mater. Interfaces 2022, 14, 17405.
- [74] a) Q. Hu, Y. He, D. Ren, Y. Song, Y. Wu, H. Liang, J. Gao, G. Xu, J. Cai, T. Li, H. Xu, L. Wang, Z. Chen, X. He, Nano Energy 2022, 96, 107123; b) X.-D. Zhang, J.-L. Shi, J.-Y. Liang, Y.-X. Yin, J.-N. Zhang, X.-Q. Yu, Y.-G. Guo, Adv. Mater. 2018, 30, 1801751; c) F. Zheng, C. Yang, X. Xiong, J. Xiong, R. Hu, Y. Chen, M. Liu, Angew. Chem. **2015**, 54, 13058.
- [75] a) X. Zhang, I. Belharouak, L. Li, Y. Lei, J. W. Elam, A. Nie, X. Chen, R. S. Yassar, R. L. Axelbaum, Adv. Energy Mater. 2013, 3, 1299; b) Y.-K. Sun, M.-J. Lee, C. S. Yoon, J. Hassoun, K. Amine, B. Scrosati, Adv. Mater. 2012, 24, 1192; c) Y. Cho, Y.-S. Lee, S.-A. Park, Y. Lee, J. Cho, Electrochim. Acta 2010, 56, 333.
- [76] F. Strauss, J. H. Teo, J. Maibach, A. Y. Kim, A. Mazilkin, J. Janek, T. Brezesinski, ACS Appl. Mater. Interfaces 2020, 12, 57146.
- [77] M. Zhao, Q. Chen, Ionics 2021, 27, 961.
- [78] W. Lv, J. Gu, Y. Niu, K. Wen, W. He, J. Electrochem. Soc. 2017, 164, A2213.
- [79] A. Schiele, B. Breitung, A. Mazilkin, S. Schweidler, J. Janek, S. Gumbel, S. Fleischmann, E. Burakowska-Meise, H. Sommer, T. Brezesinski, ACS Omega 2018, 3, 16706.

- [80] W. Li, X. Li, M. Chen, Z. Xie, J. Zhang, S. Dong, M. Qu, Electrochim. Acta 2014, 139, 104.
- [81] a) K. Zhao, C. Wang, Y. Yu, M. Yan, Q. Wei, P. He, Y. Dong, Z. Zhang, X. Wang, L. Mai, Adv. Mater. Interfaces 2018, 5, 1800848; b) C.-F. Lin, A. C. Kozen, M. Noked, C. Liu, G. W. Rubloff, Adv. Mater. Interfaces 2016, 3, 1600426; c) C. Zhu, K. Han, D. Geng, H. Ye, X. Meng, Electrochim. Acta 2017, 251, 710.
- [82] X. Xiao, M. W. Verbrugge, J. S. Wang (Google Patents) United States, 2016.
- [83] X. Teng, C. Zhan, Y. Bai, L. Ma, Q. Liu, C. Wu, F. Wu, Y. Yang, J. Lu, K. Amine, ACS Appl. Mater. Interfaces 2015, 7, 22751.
- [84] S. Klein, S. van Wickeren, S. Röser, P. Bärmann, K. Borzutzki, B. Heidrich, M. Börner, M. Winter, T. Placke, J. Kasnatscheew, Adv. Energy Mater. 2021, 11, 2003738.
- [85] D. Goers, M. Holzapfel, W. Scheifele, E. Lehmann, P. Vontobel, P. Novák, J. Power Sources 2004, 130, 221.
- [86] M. Lanz, P. Novák, J. Power Sources 2001, 102, 277.
- [87] R. Nozu, E. Suzuki, O. Kimura, N. Onagi, T. Ishihara, Electrochim. Acta 2020, 332, 135238.
- [88] I. A. Shkrob, T. W. Marin, Y. Zhu, D. P. Abraham, J. Phys. Chem. C 2014. 118. 19661.
- [89] H.-B. Han, S.-S. Zhou, D.-J. Zhang, S.-W. Feng, L.-F. Li, K. Liu, W.-F. Feng, J. Nie, H. Li, X.-J. Huang, M. Armand, Z.-B. Zhou, J. Power Sources 2011, 196, 3623.
- [90] Z.-B. Zhou, M. Takeda, T. Fujii, M. Ue, J. Electrochem. Soc. 2005, 152. A351.
- [91] Y. Chikaoka, E. Iwama, S. Seto, Y. Okuno, T. Shirane, T. Ueda, W. Naoi, M. T. H. Reid, K. Naoi, Electrochim. Acta 2021, 368,
- [92] S. Jiao, X. Ren, R. Cao, M. H. Engelhard, Y. Liu, D. Hu, D. Mei, J. Zheng, W. Zhao, Q. Li, N. Liu, B. D. Adams, C. Ma, J. Liu, J.-G. Zhang, W. Xu, Nat. Energy 2018, 3, 739.
- [93] X. Shangguan, G. Xu, Z. Cui, Q. Wang, X. Du, K. Chen, S. Huang, G. Jia, F. Li, X. Wang, D. Lu, S. Dong, G. Cui, Small 2019, 15, 1900269.
- [94] a) X.-B. Cheng, R. Zhang, C.-Z. Zhao, F. Wei, J.-G. Zhang, Q. Zhang, Adv. Sci. 2016, 3, 1500213; b) A. M. Haregewoin, A. S. Wotango, B.-J. Hwang, Energy Environ. Sci. 2016, 9, 1955; c) S. S. Zhang, J. Power Sources 2006, 162, 1379; d) H. Zhao, Y. Qian, S. Hu, G. Luo, C. Nie, P. Qiu, Y. Kang, H. Wang, Y. Chu, Q. Wang, J. Wang, H. Shao, K. Xu, Y. Deng, ACS Appl. Mater. Interfaces 2021, 13, 29676; e) J. Zheng, M. H. Engelhard, D. Mei, S. Jiao, B. J. Polzin, J.-G. Zhang, W. Xu, Nat. Energy 2017, 2, 17012.
- [95] a) J. E. Harlow, X. Ma, J. Li, E. R. Logan, Y. Liu, N. Zhang, L. Ma, S. L. Glazier, M. M. E. Cormier, M. Genovese, S. Buteau, A. Cameron, J. E. Stark, J. R. Dahn, J. Electrochem. Soc. 2019, 166, A3031; b) E. R. Logan, H. Hebecker, X. Ma, J. Quinn, Y. Hyeleong, S. Kumakura, J. Paulsen, J. R. Dahn, J. Electrochem. Soc. 2020, 167, 060530; c) W. G. Song, J. Harlow, E. R. Logan, H. Hebecker, M. Coon, L. Molino, M. Johnson, J. R. Dahn, M. Metzger, J. Electrochem. Soc. 2021, 168, 090503; d) T. Taskovic, L. M. Thompson, A. Eldesoky, M. D. Lumsden, J. R. Dahn, J. Electrochem. Soc. 2021, 168, 010514; e) X. Ma, R. S. Young, L. D. Ellis, L. Ma, J. Li, J. R. Dahn, J. Electrochem. Soc. 2019, 166, A2665.
- [96] X. Wu, S. Lou, X. Cheng, C. Lin, J. Gao, Y. Ma, P. Zuo, C. Du, Y. Gao, G. Yin, ACS Appl. Mater. Interfaces 2018, 10, 27056.
- [97] a) C. H. Jung, D. H. Kim, D. Eum, K. H. Kim, J. Choi, J. Lee, H. H. Kim, K. Kang, S. H. Hong, Adv. Funct. Mater. 2021, 31, 2010095; b) D.-H. Kim, J.-H. Song, C.-H. Jung, D. Eum, B. Kim, S.-H. Hong, K. Kang, Adv. Energy Mater. 2022, 12, 2200136; c) D. Kong, J. Hu, Z. Chen, K. Song, C. Li, M. Weng, M. Li, R. Wang, T. Liu, J. Liu, M. Zhang, Y. Xiao, F. Pan, Adv. Energy Mater. **2019**. 9. 1901756.
- [98] a) B. Qiu, M. Zhang, L. Wu, J. Wang, Y. Xia, D. Qian, H. Liu, S. Hy, Y. Chen, K. An, Y. Zhu, Z. Liu, Y. S. Meng, Nat. Commun. **2016**, 7, 12108; b) S. Ramakrishnan, B. Park, J. Wu, W. Yang,



ADVANCED FUNCTIONAL 16163028, 2022, 47, Downloaded from https://advanced.onlinelibrary.wiley.com/doi/10.1002/adfm.202208586 by University Town Of Shenzhen, Wiley Online Library on [2311/2025]. See the Terms

and-conditions) on Wiley Online Library for rules of use; OA articles are governed by the applicable Creative Commons

www.advancedsciencenews.com www.afm-journal.de

- B. D. McCloskey, *J. Am. Chem. Soc.* **2020**, *142*, 8522; c) Rosy, H. Sclar, E. Evenstein, S. Haber, S. Maiti, T. Sharabani, M. Leskes, M. Noked, *Chem. Mater.* **2019**, *31*, 3840.
- [99] X. Xu, H. Huo, J. Jian, L. Wang, H. Zhu, S. Xu, X. He, G. Yin, C. Du, X. Sun, Adv. Energy Mater. 2019, 9, 1803963.
- [100] a) Y.-K. Sun, S.-T. Myung, B.-C. Park, J. Prakash, I. Belharouak, K. Amine, Nat. Mater. 2009, 8, 320; b) H. Xu, S. Li, C. Zhang, X. Chen, W. Liu, Y. Zheng, Y. Xie, Y. Huang, J. Li, Energy Environ. Sci. 2019, 12, 2991.
- [101] H. Buqa, M. Holzapfel, S. Wussler, W. Scheifele, E. Studenik, P. Blanc, 2015.
- [102] U. Mattinen, M. Klett, G. Lindbergh, R. W. Lindström, J. Power Sources 2020, 477.
- [103] S. Kozono, K. Yukimoto, S. Yamate, T. Yamafuku, Y. Katayama, A. Funabiki, T. Nukuda (GS Yuasa Corporation) Kyoto, 2011.
- [104] a) R. Petibon, C. P. Aiken, L. Ma, D. Xiong, J. R. Dahn, *Electro-chim. Acta* 2015, 154, 287; b) X. Tong, X. Ou, N. Wu, H. Wang, J. Li, Y. Tang, Adv. Energy Mater. 2021, 11, 2100151.
- [105] a) H. Seki, K. Yoshima, Y. Yamashita, S. Matsuno, N. Takami, J. Power Sources 2021, 482, 228950; b) W. D. Jung, M. Jeon, S. S. Shin, J.-S. Kim, H.-G. Jung, B.-K. Kim, J.-H. Lee, Y.-C. Chung, H. Kim, ACS Omega 2020, 5, 26015.

- [106] a) Y. G. Cho, S. H. Jung, J. Jeong, H. Cha, K. Baek, J. Sung, M. Kim,
 H. T. Lee, H. Kong, J. Cho, S. J. Kang, J. M. Park, H. K. Song, ACS
 Appl. Mater. Interfaces 2021, 13, 9965; b) S. Wang, X. Xiao, C. Fu,
 J. Tu, Y. Tan, S. Jiao, J. Mater. Chem. A 2018, 6, 4313.
- [107] a) F. Wu, G.-T. Kim, T. Diemant, M. Kuenzel, A. R. Schür, X. Gao, B. Qin, D. Alwast, Z. Jusys, R. J. Behm, D. Geiger, U. Kaiser, S. Passerini, Adv. Energy Mater. 2020, 10, 2001830; b) C. Locati, U. Lafont, C. J. Peters, E. M. Kelder, J. Power Sources 2009, 189, 454.
- [108] S. Chen, J. Zheng, D. Mei, K. S. Han, M. H. Engelhard, W. Zhao, W. Xu, J. Liu, J.-G. Zhang, Adv. Mater. 2018, 30, 1706102.
- [109] X. Cao, H. Jia, W. Xu, J.-G. Zhang, J. Electrochem. Soc. 2021, 168, 010522.
- [110] a) L. Suo, O. Borodin, T. Gao, M. Olguin, J. Ho, X. Fan, C. Luo, C. Wang, K. Xu, Science 2015, 350, 938; b) J. Hu, Y. Ji, G. Zheng, W. Huang, Y. Lin, L. Yang, F. Pan, Aggregate 2022, 3, e153; c) J. Hu, H. Guo, Y. Li, H. Wang, Z. Wang, W. Huang, L. Yang, H. Chen, Y. Lin, F. Pan, Nano Energy 2021, 89, 106413; d) J. Zheng, G. Tan, P. Shan, T. Liu, J. Hu, Y. Feng, L. Yang, M. Zhang, Z. Chen, Y. Lin, J. Lu, J. C. Neuefeind, Y. Ren, K. Amine, L.-W. Wang, K. Xu, F. Pan, Chem. 2018, 4, 2872.
- [111] Z. Chen, Y. Qin, K. Amine, Y. K. Sun, J. Mater. Chem. 2010, 20, 7606



Pei Liu is a master student at the College of Chemistry and Environmental Engineering in Shenzhen University. Her research interests mainly lie in the design and development of cathode materials, storage mechanism exploration and electrochemical performance optimization.



Jiangtao Hu received his Ph.D degree in 2018 from Peking University (China). Between 2018 and 2021, he worked with Jie Xiao in Pacific Northwest National Laboratory (PNNL, USA) as a postdoc research fellow. Prof. Hu is currently an associate professor at College of Chemistry and Environmental Engineering in Shenzhen University. His research interests mainly lie in design and development of functional materials for energy storage and conversion applications such as Li-ion battery, and Na-ion battery.

16163028, 2022, 47, Downloaded from https://advanced.onlinelibrary.wiley.com/doi/10.1002/adfm.202208586 by University Town Of Shenzhen, Wiley Online Library on [23/11/2025]. See the Terms

of use; OA articles are governed by the applicable Creative Commons License



Feng Pan, Chair-Professor, Founding Dean of School of Advanced Materials, Peking University Shenzhen Graduate School, Director of National Center of Electric Vehicle Power Battery and Materials for International Research, received his B.S. degree from Dept. Chemistry, Peking University in 1985 and Ph.D. from Dept. of P&A Chemistry, University of Strathclyde, U.K. with "Patrick D. Ritchie Prize" for the best Ph.D. in 1994. Prof. Pan has been engaged in fundamental research of structure chemistry, exploring "Material Gene" for Li-ion batteries and developing novel energy conversion-storage materials & devices. He also received the 2018 ECS Battery Division Technology Award.



Qianling Zhang received her Ph.D degree in 2001 from Sun Yat-Sen University. She is currently the professor of College of Chemistry and Environmental Engineering in Shenzhen University, Standing Director of Shenzhen Biological Medicine Promotion Association, and Member of Guangdong Inorganic Chemistry Professional Committee. In recent years, Prof. Zhang has been engaged in the design and synthesis of graphene and its composite materials and its application in energy storage and transformation.



Jianhong Liu, Professor of Shenzhen University, Executive Director of Graphene Composite Research Center of Shenzhen University, and Chairman of Shenzhen Eigen-Equation Graphene Technology Co. Ltd. Prof. Liu has published more than 200 SCI articles and 70 invention patents, and achieved more than 10 national and provincial science and technology awards. He was honored with the 4th Youth Science and Technology Award of Shenzhen and the Subsidy of Shenzhen Government in 2005, and awarded the advanced individual of "Thousand and ten Projects" of Guangdong Colleges in 2006 and identified as "High-level Talents" of Shenzhen in 2009.